

IAVCEI 2013 Field Trip Guide

A02: Unzen and Aso volcanoes, central Kyushu, Japan: Unzen's new lava dome climb and 1991-95 pyroclastic flows and Aso's active crater and one of the largest calderas in Japan

Shinji Takarada *, Yasuo Miyabuchi**, Hideo Hoshizumi*,
Takeshi Matsushima*** and Daisuke Nagai****

*: Geological Survey of Japan, AIST, Tsukuba Central 7, Higashi 1-1-1, Tsukuba 305-8567, Japan

** : Faculty of Education, Kumamoto University, Kurokami 2-40-1, Chuo-ku, Kumamoto 860-8555, Japan

***: Institute of Seismology and Volcanology, Faculty of Sciences, Kyushu University, 2-5643-26, Shinzan, Shimabara 855-0843, Japan

****: Unzen Disaster Museum, Heisei-cho 1-1, Shimabara 855-0879, Japan

1. Introduction and aim of trip

Intense volcanic activities have continued since late Pliocene in central Kyushu, southwestern Japan. Numerous explosive and effusive eruptions occurred in this volcanic field. Aso and Unzen volcanoes are the most active in this region. This field excursion will focus on eruptive history of Aso Volcano, and the 1991 to 1995 pyroclastic flows, new Heisei-Shinzan lava dome, and recent eruptions at Unzen Volcano. Volcanic activities during caldera-forming stage and post-caldera activities, petrology, and recent eruptions at Aso Volcano are described in Ch. 2. Geology of eruptive history, geophysics, 1990-95 eruptions and disasters at Unzen Volcano are described in Ch. 3. Guide to the field stops at Aso Volcano (day 1 and 2) and Unzen Volcano (days 3, 4 and 5) are described in Ch. 4.

Aso Volcano, which is located in central Kyushu (Fig. 1), is one of the most beautiful caldera volcanoes in the world (Fig. 2). Aso is a symbol of Kumamoto Prefecture, therefore Kumamoto has been called Hi-no-kuni, which means the fire country. In 1934 Aso Volcano and the adjacent Kuju Volcano (10 km NE) were designated as one of Japan's national parks. The Aso region is one of the most popular tourist destinations in Kyushu for its spectacular volcanic views and hot springs.

During 270 to 90 ka (Matsumoto *et al.*, 1991), gigantic pyroclastic-flow eruptions of andesitic to rhyolitic magma occurred four times in the volcanic field and formed the Aso caldera, 25 km north-south and 18 km east-west in diameter. Post-caldera central cones initiated their eruptive activity soon after the last caldera-forming eruption (90 ka) and have produced large volumes of fallout tephra layers and lava flows. Nakadake Volcano, which is the only active central cone, is one of the most active volcanoes in Japan. Its recent activity is

characterized by ash and strombolian eruptions and phreatic or phreatomagmatic explosions. This fieldtrip will focus on gigantic pyroclastic-flow deposits related to the caldera formation and explosive and effusive post-caldera activity of the volcano. We will also discuss recent activity of Aso Volcano and its hazard assessments (days 1 and 2).

Unzen Volcano field excursion will focus on the 1991 to 1995 pyroclastic flows produced by dome collapse, a new lava dome (Heisei-Shinzan), and the growth history of Unzen Volcano (Takarada *et al.*, 2007). Depositional features, the emplacement process, and disasters resulting from the pyroclastic flows/surges and lahars will be discussed on July 17 (day 3). On July 18 (day 4), we will climb to the top of the new lava dome, observe its growth pattern, and discuss the degassing mechanism. The growth history of Unzen Volcano, starting from 500 ka, will be examined on July 19 (day 5). The 1792 Mayuyama debris avalanche deposit (produced the worst volcanic disaster in Japan, killing 15,000 people) will also be visited. In 2009, Unzen Volcano area, was certified to the world Geopark for the first time in Japan. There are many geosites in the Shimabara Peninsula including Unzen Volcano. Tourists learn about science of volcanoes and disaster prevention in this Geopark.

2. Aso Volcano

2-1. Outline of geologic setting

Late Cenozoic volcanic activity in central and southern Kyushu resulted from the subduction of Philippine Sea Plate (7 Ma). The present volcanic front was established about 2Ma. Extensive plateaus of large-scale pyroclastic flow deposits are

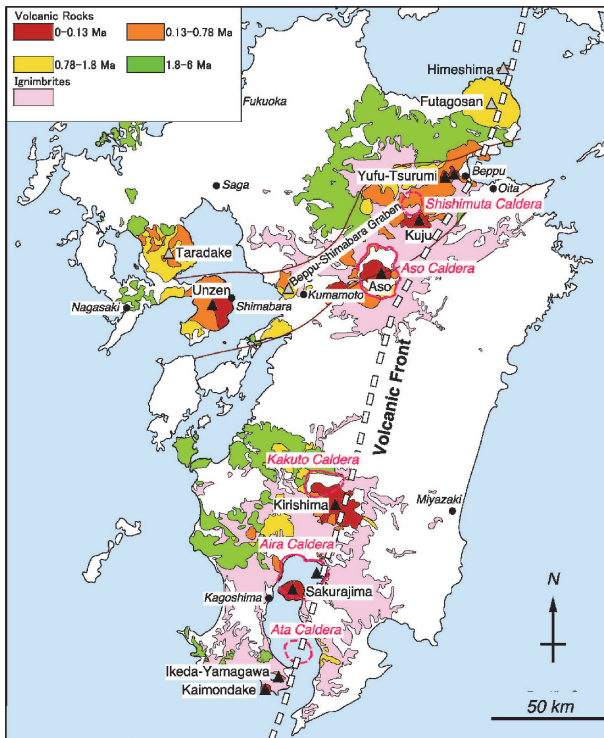


Figure 1. Map showing distribution of volcanic products in Kyushu and the volcanic front (simplified from Geological Survey of Japan, 1992). Aso and Unzen volcanoes are located in the central part of Kyushu.

distributed around large calderas in central and southern Kyushu, located on the volcanic front (Fig. 1, Aso, Aira, Ata, and Kikai calderas).

Intense volcanic activity occurred in central Kyushu through late Pliocene to early Pleistocene. Basement rocks of the volcanic field are composed mainly of Paleozoic to Mesozoic formations, their metamorphic equivalents and Cretaceous granites (Ono *et al.*, 1981). The basement of Aso Volcano was confirmed to lie at shallow depths between 150 and 500 m from the caldera floor near the caldera wall (Watanabe and Ono, 1992). In a period from about 3 to 0.4 Ma, large amounts of lava and pyroclastics were erupted from many eruption centers in the Aso region prior to the activity of Aso Volcano. The rocks during the period are called Pre-Aso volcanic rocks, and are composed mainly of pyroxene andesite with subordinate amounts of hornblende andesite, biotite rhyolite and basalt (Ono, 1965). Some of them are exposed in the caldera wall.



Figure 2. Oblique view of Aso caldera and post-caldera central cones from the south.

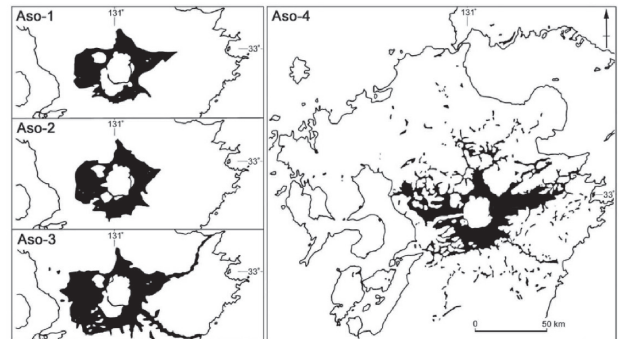


Figure 3. Distribution of Aso pyroclastic flow deposits (Ono and Watanabe, 1983).

2-2. Caldera-forming stage eruptions

Four major explosive eruptions occurred from 270 to 90 ka, and these produced voluminous pyroclastic flows that covered much of central Kyushu (Fig. 3). The Aso pyroclastic flow deposits were divided into four units: Aso-1 (270 ka), Aso-2 (140 ka), Aso-3 (120 ka) and Aso-4 (90 ka) in ascending order (Ono *et al.*, 1977). The flows successively flowed into valleys between basement mountains, filled them up and formed pyroclastic-flow plateaus. The slopes of the surface of the plateaus are less than 1° to 2° . Between each of the four large eruptive units, pyroclastic eruptions produced fallout tephra layers. Nekodake, formerly thought to be a post-caldera central cone, is now interpreted to be a deeply dissected stratovolcano near the eastern rim of the caldera between the Aso-2 and Aso-3 eruptions (Ono and Watanabe, 1985; Matsumoto *et al.*, 1991).

The total volume of four gigantic pyroclastic flow deposits from Aso Volcano is estimated at more than 300 km^3 . The Aso-4 eruption about 90 ka

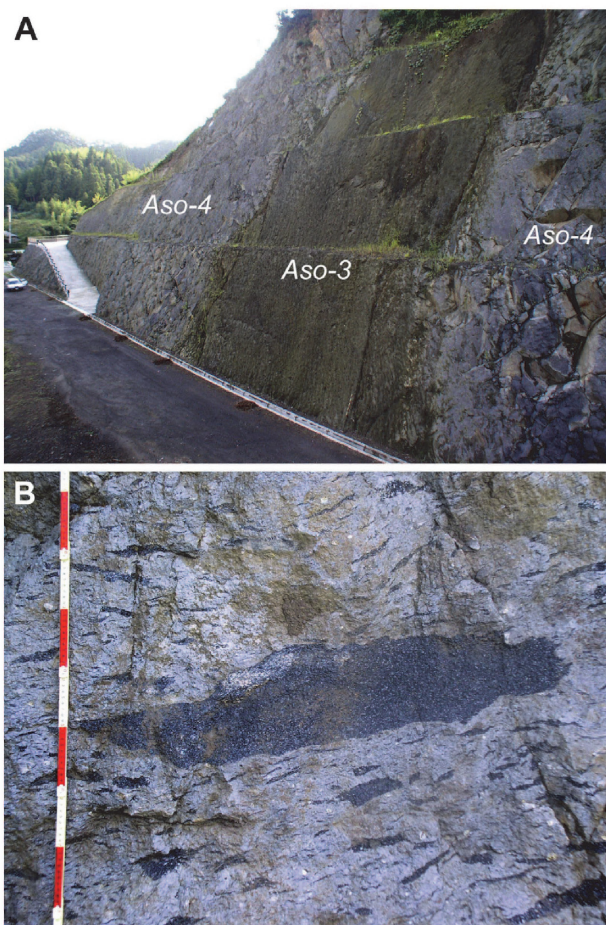


Figure 4. Photographs of the Aso-4 pyroclastic flow deposit. (A) Densely-welded Aso-4 pyroclastic flow deposit overlying Aso-3 pyroclastic flow deposit at Taketa City, ca. 20 km east of Aso caldera. (B) A huge pumice lens included in the welded Aso-4 pyroclastic flow deposit. Scale segments are 10 cm.

is the largest scale eruption at Aso Volcano, and consists of several flow units (Watanabe, 1978). The Aso-4 pyroclastic-flow deposits (Fig. 4) with a volume of more than 80 km³ cover most part of central Kyushu (Watanabe, 2001), and the flows ran across the sea and reached an area about 150 km from the source (Ono and Watanabe, 1983). A co-ignimbrite ash fall deposit associated with the Aso-4 pyroclastic flow is one of the key widespread tephra layers in Japan. It covers all of Japan and is seen in eastern Hokkaido (northeastern end of Japan), about 1,700 km from Aso Volcano (Machida *et al.*, 1985).

Aso caldera, 25 km north-south and 18 km east-west in diameter, was formed by the four large eruptions. The shape of the caldera rim is very complicated with many embayments and promontories (Fig. 2). Data from drill holes and

Bouguer anomalies suggest that the size of original collapse was much smaller than the present topographic depression. The present outline of the caldera probably resulted from enlargements by landslides which occurred soon after the original collapse (Ono and Watanabe, 1983).

2-3. Post-caldera activity

Post-caldera cones have arisen near the center of the caldera since the Aso-4 eruption at ca. 90 ka (Ono and Watanabe, 1985). The central cones have produced voluminous fallout tephra layers and lava flows. At least seventeen cones are visible on the surface (Fig. 5), but many more edifices, consisting of both lava and pyroclastics, have been detected under the present central cones by bore holes (Uto *et al.*, 1994; Hoshizumi *et al.*, 1997). The shapes and structures of the central cones vary depending on their chemistry, which ranges from basalt to rhyolite (Ono and Watanabe, 1985). Takanoobane lava dome (568 m a.s.l.; Watanabe, 2001) of biotite rhyolite was constructed near the west rim of the caldera at 51 ka (Matsumoto *et al.*, 1991). Kusasenrigahama Volcano of pyroxene dacite is a welded pumice cone with a 1 km-across crater and produced one of the largest plinian pumice fall deposits of the central cones about 30 ka (Miyabuchi *et al.*, 2003). Eboshidake (1,337 m) and Okamadoyama (1,153 m) are stratovolcanoes of pyroxene andesite. Yomineyama (913 m), Washigamine, Naraodake (1,331 m) and Takadake (1,592 m: the highest peak of Aso Volcano) are stratovolcanoes of olivine-pyroxene andesite to basalt. They are composed of piles of agglutinate or welded spatter near the summits and lava flows near their bases.



Figure 5. Oblique aerial view of the central part of post-caldera central cones of Aso Volcano.

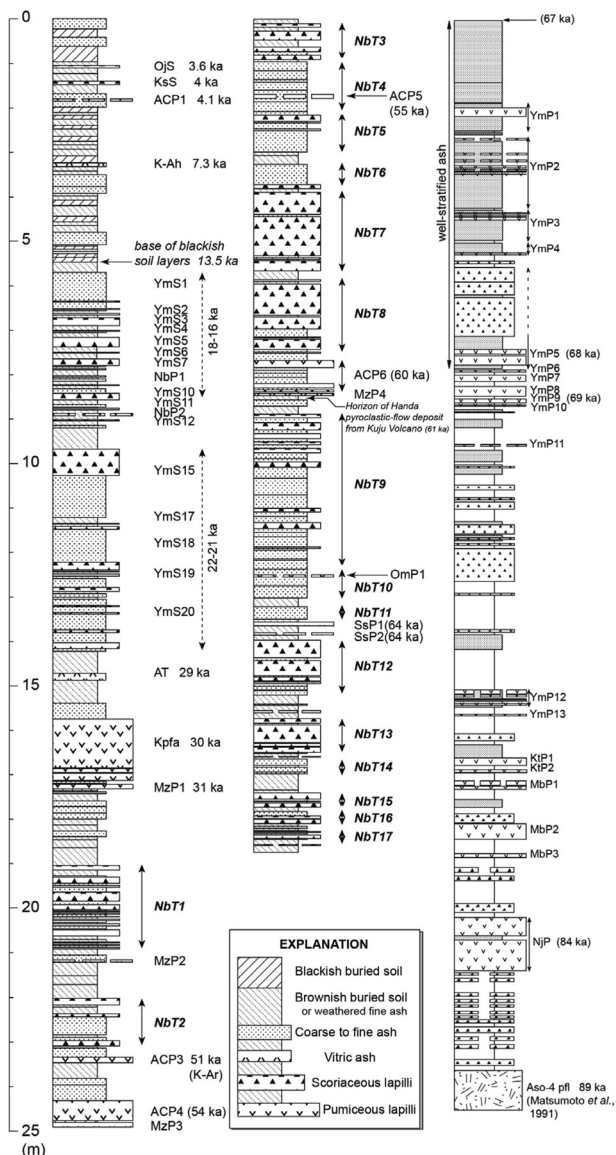


Figure 6. Generalized composite stratigraphy of tephra layers from post-caldera central cones of Aso Volcano during the past 90,000 years at the east of Aso caldera (modified from Miyabuchi, 2009, 2011). Ages of tephra were determined by calibrated ^{14}C dates (Miyabuchi, 2009; Okuno, 2002) and K-Ar dates (Matsumoto *et al.*, 1991) and ages in parentheses were estimated by their stratigraphic positions.

Janoo (754 m), Kishimadake (1,326 m), Ojodake (1,238 m) and Komezuka (954 m) are Holocene scoria cones of pyroxene-olivine basalt. Kishimadake and Ojodake Volcanoes produced subplinian scoria fall deposits and lava flows about 4 and 3.6 ka (Miyabuchi and Watanabe, 1997; Miyabuchi, 2009).

Nakadake Volcano (1,506 m) is the only active central cone in Aso caldera, and is a composite volcano of basaltic andesite to basalt. Nakadake became active from ca. 22-21 ka (Miyabuchi *et al.*,

2004a), and has formed an old edifice (agglutinate and lava), a young edifice (pyroclasts and lava) and a younger pyroclastic cone (Ono and Watanabe, 1985). The old volcanic edifice is the main cone of Nakadake Volcano, rising about 900 m from the caldera floor. The upper part of the edifice is a complex cone made largely of welded spatter, with subordinate amounts of other pyroclastic materials. The lower part of the edifice is composed mainly of lava flows. Recent tephrochronological studies (Miyabuchi *et al.*, 2003, 2004a) indicate that most of the edifice was constructed at ca. 22-21 ka. Thereafter, the western half of the upper edifice was destroyed by a northwestward-directed horseshoe-like collapse, leaving a 250-m-high collapsed crater wall (Ono *et al.*, 1995). The young volcanic edifice is believed to have formed during Holocene time, and the youngest pyroclastic cone subsequently rose inside the young edifice (Ono and Watanabe, 1985).

The stratigraphy and chronology of tephra layers have been evaluated through study of the thick tephra sequence preserved mainly atop the Aso pyroclastic-flow plateau around the caldera in order to re-construct the eruptive history of post-caldera central cones of Aso Volcano during the past 90,000 years (Miyabuchi, 2009, 2011). Most of the tephra layers distributed in and around Aso caldera are andesitic to basaltic-andesitic scoria-fall and ash-fall deposits. Their stratigraphy is very complicated because they are apparently so similar that it is difficult to distinguish each scoria-fall layers in the field. However, dacitic to rhyolitic pumice-fall deposits from some central cones interbedded with the tephra layers are very useful for correlation of stratigraphic units at separated localities. Therefore, the pumice-fall deposits are used in order to construct the tephrostratigraphy and eruptive history of post-caldera central cones during the past 90,000 years (Fig. 6). Thirty-six pumice-fall deposits were identified including fifteen major key beds (Miyabuchi *et al.*, 2003). In ascending order they are Nojiri pumice (NjP), Ogashiwa pumice (OgP), Yamasaki pumice 5 to 1 (YmP5-YmP1), Sasakura pumice 2 (SsP2) and 1 (SsP1), Aso central cone pumice 6 to 3 (ACP6-ACP3), Kusanenrigahama pumice (Kpfa), and Aso central cone pumice 1 (ACP1). Phenocrystic minerals of most pumices are

plagioclase, ortho- and clinopyroxene and titanomagnetite, but NjP, ACP5, ACP3, and ACP1 include biotite, and NjP and SsP2 contain hornblende phenocrysts. ACP4 and ACP3 were correlated, respectively, with the dacitic Tateno lava and the rhyolitic Takanoobane lava (51 ka; K-Ar age) distributed in the western part of the central cones (Miyabuchi *et al.*, 2004b, 2004c).

On the basis of the reconstructed tephrostratigraphy (Miyabuchi, 2009, 2011), the eruptive history of Aso Volcano during the past 90,000 years is interpreted as follows.

The post-caldera central cones must have been emplaced soon after the last caldera-forming eruption (Aso-4 eruption; 89 ka) because several tephra layers occur soon after the Aso-4 pyroclastic-flow deposit. Between 89 and 68 ka, minor pumice- and scoria-fall deposits were produced intermittently, together with two large pumice-fall deposits: the NjP (VEI 4-5; Volcanic Explosivity Index; Newhall and Self, 1982) and the OgP (VEI 4; distributed only NE of caldera). Their sources are believed to be edifices formed during the early stage of the post-caldera central cone emplacement, which are now buried under the present central cones (Uto *et al.*, 1994; Watanabe, 2001). A series of violent eruptions occurred between 68 and 67 ka that emplaced well-stratified ash layers, which can be easily traced around the Aso caldera, including scoria and thick pumice beds. These deposits are subdivided into five units (YmP5-YmP1 in ascending order) by four thin soil beds indicating short time intervals. The total volume of the YmP5-YmP1 sequence is approximately 4 km³.

After 67 ka, intermittent explosive mafic eruptions produced several poorly-vesiculated scoria- and lithic-fall deposits, which are distributed mainly to the east of the caldera. Two large pumice-fall deposits were erupted: the hornblende-rich SsP2 (VEI 3) and the obsidian-rich SsP1 (VEI 3) at 64 ka. Thereafter, violent eruptions through to 61 ka emplaced a thick alternating sequence of ash and scoria beds around the Aso caldera. A series of eruptions produced a plinian pumice-fall deposit (KjP1) at 61 ka, and the Handa pyroclastic-flow deposit occurred at Kuju Volcano (ca. 10 km NE of Aso Volcano) at the same time.

The ACP6 tephra (VEI 4), which is an alternating sequence of pumice and ash beds, was erupted at 60 ka soon after the Handa pyroclastic-flow eruption. The ACP6 eruption is followed by the largest scoria eruptions of post-caldera activity at Aso Volcano. Subsequently, ash-producing eruptions occurred intermittently including the biotite-rich ACP5 (VEI 4), ejected at 55 ka.

Two large silicic eruptions occurred without a long dormancy in the western part of Aso caldera at 51 ka. Both eruptions were initiated by plinian eruptions and were followed by compositionally homogeneous lava flows. At first a dacitic eruption produced a plinian pumice-fall deposit (ACP4; VEI 4) followed by extrusion of a dacitic lava flow (Tateno lava; ca. 0.45 km³; Miyabuchi *et al.*, 2004c). This lava filled the Tateno Gorge, which is the only outlet of Aso caldera, resulting in the formation of a lake inside the caldera. Immediately after the Tateno eruption, a biotite-rhyolitic eruption occurred at Takanoobane Volcano and produced a plinian pumice-fall deposit (ACP3; VEI 4) followed by extrusion of the homogeneous Takanoobane lava flow. This eruption formed a distinct lava dome at the source.

Between 51 and 32 ka, eruptions emitted minor scoria- and ash-fall deposits intermittently. Eboshidake Volcano, which is a pyroxene-andesitic stratovolcano located at the southern edge of Kusasenrigahama crater, extruded lava flows and formed its edifice mostly of agglutinate at ca. 40 ka (Miyabuchi *et al.*, 2004c). Eruptive activity was then relatively calm between 32 and 31 ka. During this calm period Sasa (a dwarf bamboo) grassland was developed around the Aso caldera and a widespread humic black soil layer was formed (Miyabuchi *et al.*, 2012).

The catastrophic 30 ka eruption at Kusasenrigahama crater was initiated by the dacitic Sawatsuno lava flow (Miyabuchi *et al.*, 2004c). The lava extrusion was followed by the largest plinian pumice-fall deposit during the post-caldera stage (Kpfa: 2.2 km³). This explosive eruption supposedly destroyed the northern part of the Eboshidake Volcano edifice. Volcanic activity then waned after the Kusasenrigahama eruption.

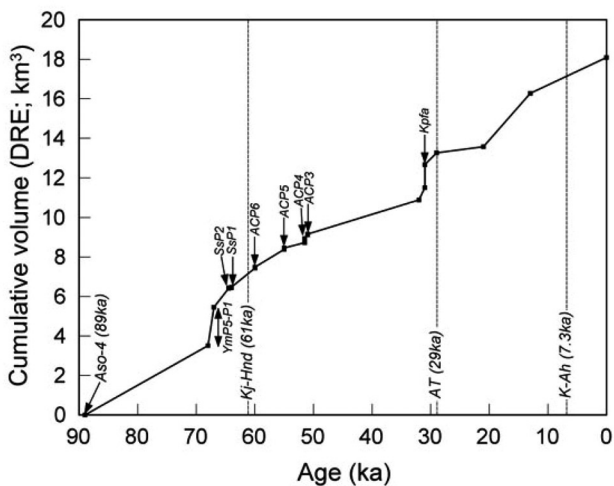


Figure 7. Cumulative erupted volume versus time for fallout tephra layers in the post-caldera stage of Aso Volcano.

Nakadake Volcano, the only active central cone of Aso caldera, was then initiated around 22-21 ka. In its initial stage, multiple sub-plinian and violent ash-emitting eruptions occurred intermittently, forming thick alternating beds of scoria and ash (YmS20-YmS15 in ascending order) around Aso caldera (Miyabuchi *et al.*, 2004a). The Nakadake Volcano apparently produced lava flows to the north and south of the vent, and formed an edifice composed of lavas and agglutinates (welded scoria-fall deposits) known as the Nakadake old edifice (Ono and Watanabe, 1985). It is presumed that most of the old edifice of the volcano was constructed during this period. A bomb-rich basaltic pyroclastic-flow deposit probably generated by an explosion of the semi-solidified lava lake or conduit, descended the northeastern flank of Nakadake at 19 ka (Miyabuchi *et al.*, 2006). Thereafter, intermittent sub-plinian and ash-emitting mafic eruptions occurred in the period between 18-16 ka (Miyabuchi *et al.*, 2004a).

The activity of Nakadake Volcano waned around 13.5 ka. Its most characteristic volcanic activity in Holocene time has been ash eruptions, which have formed a continuous fallout of black sandy ash from dark eruption plumes (Ono *et al.*, 1995). The ACP1 (biotite-rich pumice) was erupted from an unknown vent in the northwestern part of the central cones at 4.1 ka. Two sub-plinian eruptions producing scoria-fall deposits traced to the east of Aso caldera occurred at Kishimadake (4 ka) and Ojodake (3.6 ka) and were followed by

compositionally homogeneous lava flows (Nakamura and Watanabe, 1995; Miyabuchi and Watanabe, 1997). Furthermore, a strombolian eruption and lava extrusion formed Komezuka scoria cone at 3.3 ka (Miyabuchi, 2010). Although the frequency of explosive eruptions at Nakadake has been relatively low, a large phreatomagmatic eruption occurred at 1.5 ka and produced a poorly-sorted scoria-fall deposit (N2S; Miyabuchi and Watanabe, 1997). Thereafter, Nakadake Volcano continued its activity to the present time, intercalated with short dormant periods.

A few geothermal fields exist in the western part of the post-caldera central cones. At least two phreatic eruptions produced ejecta in the order of 105 m³, at Jigoku spa in the last 10,000 years (Miyabuchi and Watanabe, 2000). A small phreatic eruption occurred at Yunotani spa in June 1816 (Ikebe and Fujioka, 2001). These phreatic eruptions provide important information for volcanic hazards in areas other than Nakadake.

Total tephra volume in the past 90,000 years is estimated at about 18.1 km³ (dense rock equivalent: DRE; Fig. 7), whereas total volume for edifices of the post-caldera central cones is calculated at about 112 km³, which is six times greater than the former. Therefore, the average magma emission rate for the past 90 ka at Aso Volcano is estimated at about 1.5 km³/ky (Miyabuchi *et al.*, 2003), which is similar to rates for other Quaternary volcanoes in Japan.

2-4. Petrology of Aso volcanic rocks

The rocks of Aso Volcano, from both the caldera-forming and post-caldera stages, have a wide compositional range from basalt to rhyolite and are chemically and mineralogically distinct from rocks of either Pre-Aso volcanic rocks exposed at the caldera wall or coeval nearby volcanoes. They are characterized by a high alkali content, especially K₂O (Ono, 1989). The caldera-forming stage rocks are predominantly silicic with some rocks of intermediate composition and minor amounts of mafic rocks (Ono *et al.*, 1981). Not only the rocks of the caldera-forming stage but those of each major eruption also range widely in chemistry. The SiO₂ contents of pumice or essential blocks in each caldera-forming stage are 65 wt.% for Aso-1, 66-58 wt.% for Aso-2, 69-56 wt.% for Aso-3 and 70-50

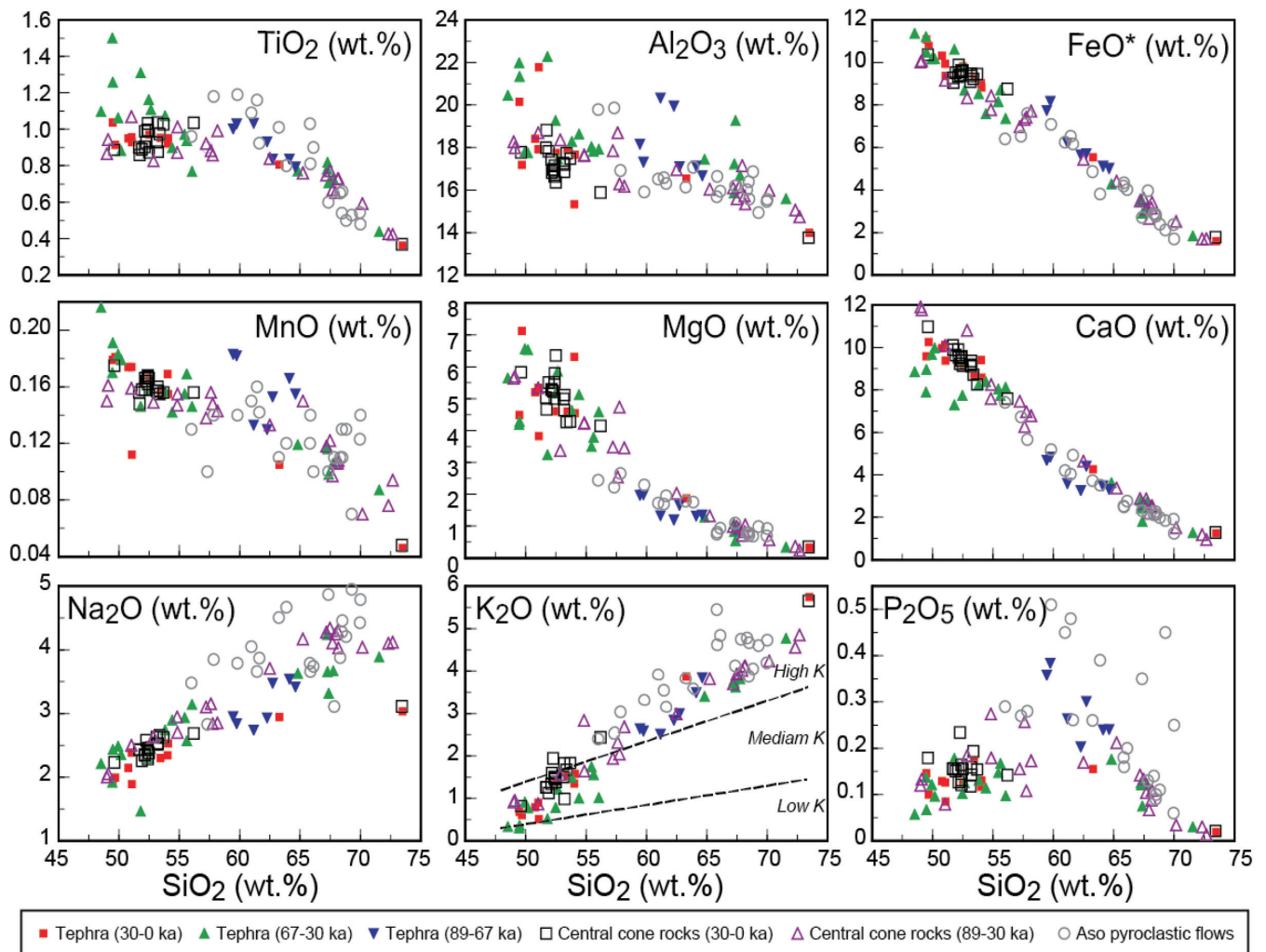


Figure 8. SiO_2 variation diagrams for major elements of tephra and rocks of Aso Volcano corresponding to whole-rock composition (Miyabuchi, 2011). Data for Aso pyroclastic flow deposits are from Ono *et al.* (1977).

wt.% for Aso-4. The fact that usually silicic rocks are erupted in earlier stages of one caldera-forming eruption while mafic rocks dominate the later stage, and that a similar sequence is followed in the next eruption suggests the presence of a zoned magma chamber and its generation within an interval of two eruptions, probably over a few tens of thousand years (Ono *et al.*, 1981).

In respect to edifices (lavas and agglutinates) of the post-caldera central cones, rocks older than 30 ka are compositionally variable ($\text{SiO}_2=48-74$ wt.%), whereas rocks younger than 30 ka are dominantly of mafic composition ($\text{SiO}_2=49-56$ wt.%) except for the rhyolitic Otogase lava (Fig. 8). This compositional trend had been previously recognized by Miyoshi *et al.* (2005). However, the tephra fallout deposits originating from the post-caldera cones between 89 and 67 ka occupy a relatively

narrow range ($\text{SiO}_2=59-65$ wt.%). Tephra beds in the period of 67-30 ka are bimodal in composition: both mafic tephra ($\text{SiO}_2=48-56$ wt. %) and silicic tephra ($\text{SiO}_2=65-72$ wt.%). Explosive eruptions producing mafic tephra ($\text{SiO}_2=49-54$ wt.%) are dominant after 30 ka. Thus, the chemical compositions of magma related to explosive and effusive eruptions of post-caldera central cones vary between ages.

The phenocrystic mineral assemblage is rather simple. Most of the rocks of Aso Volcano contain plagioclase, clinopyroxene, orthopyroxene and titanomagnetite as phenocryst (Ono and Watanabe, 1985). Some mafic rocks contain olivine phenocryst. Hornblende phenocrysts appear only in all the rocks of Aso-4 and a dacitic lava (Honzuka lava) and some pumice-fall deposits at post-caldera stage (Miyabuchi *et al.*, 2003). Biotite phenocrysts are

present only in two rhyolitic lavas (Takanoobane and Nakahoono lava; Masuda *et al.*, 2004) at the post-caldera stage.

2-5. Recent eruptions and volcanic hazards

Historic and recent activity of Nakadake

Nakadake, the only active Central Cone, has the longest documented volcanic history (Japan Meteorological Agency, 1991; Watanabe, 2001). Since AD 553, more than 100 eruptions have been documented in historical records, making Nakadake one of the most active volcanoes in Japan. The active crater of Nakadake, formed in the youngest pyroclastic cone, is composed of seven craterlets aligned from north to south. Only the northernmost crater (first crater) has been active in the past 80 years, although some others were active before the 1933 eruption. The Nakadake first crater is occupied by a hyperacidic (pH=0.43) crater lake during its calm periods (Miyabuchi and Terada, 2009) and has maintained a high heat discharge rate of approximately 220 MW (Terada *et al.*, 2008). During active periods, volcanic activity of Nakadake is characterized by continuous fallout of black sandy ash from a dark eruption plume. The ash is derived from the solid glassy top of a magma column, and is transported by a gas stream from below the solid top. This type of eruption is called an ash eruption (Ono *et al.*, 1995). In more active periods, strombolian eruptions have occurred, scattering red hot scoria clasts around the vent. Occasional phreatomagmatic explosions eject coarse lithic blocks, which are likely to cause human casualties or damage buildings near the crater and generate small, low-temperature pyroclastic flows (Ono *et al.*, 1982).

Measures against disasters

Nakadake is a very exceptional volcano because the crater area is easily accessible by a toll road and a cable car. About one million tourists visit there all year round. Ropeway stations and some restaurants are located within 1 km of the crater. The Aso Volcano Hazard Committee composed of local governments, police and fire stations was established in 1967 and published a hazard map in 1995. The committee restrains visitors to enter the crater area according to levels of volcanic activity. Even during dormant periods, the content of

volcanic gas (mainly SO₂) has been monitored automatically by five sensors since 1998, and an alarm is sounded if the gas concentration is high enough to present a hazard. The crater area is divided into five zones. Entering each zone is prohibited when the monitored concentration of SO₂ is more than 5 ppm. Consequently no persons have been killed by volcanic gas since 1998. Furthermore, Aso Volcano Museum installed a small hospital having resident nurses in September 2006.

A few hot spring resorts exit at the western part of post-caldera central cones. A small phreatic eruption occurred at Yunotani spa in June 1816 (Ikebe and Fujioka, 2001). At least two phreatic eruptions producing ejecta at an order of 105 m³ occurred at Jigoku spa in the last 10,000 years (Miyabuchi and Watanabe, 2000). These phreatic eruptions provide important information for volcanic hazards in areas other than Nakadake.

Since 1953, large-volume lahars originating from landslides have been generated by four episodes of torrential rainfall in the Aso caldera region. The June 29, 2001 sediment disaster at Aso Volcano highlights the hazard of lahars originating from landslides (Miyabuchi and Daimaru, 2004). The rupture surfaces of most landslides following the June 29, 2001 rainfall were formed at the horizon of a tephra about 3,000 years in age, the same rupture surface for landslides occurring in June 1953, July 1990 and July 2012 (Miyabuchi, 2012). Thus, tephra layers that accumulated over the past 3,000 years have collapsed following intense rainfall in the Aso caldera region. The tephra (3 ka to present), which transforms to sliding and flowing material, is distributed as an ellipse with its long axis running east-northeast from the active Nakadake crater. The landslides in 1953 (e.g. Kawaguchi and Namba, 1954), in 1990 (Kumamoto District Forest Office and Japan Forest Engineering Consultants, 1991) and in 2001 were mainly in areas where the tephra that accumulated over the past 3,000 years is more than 2 m thick. These areas therefore have great potential to generate future non-eruption-related landslides and lahars, although this will depend not only on the thickness of the tephra but also on local topography and future rainfall conditions.

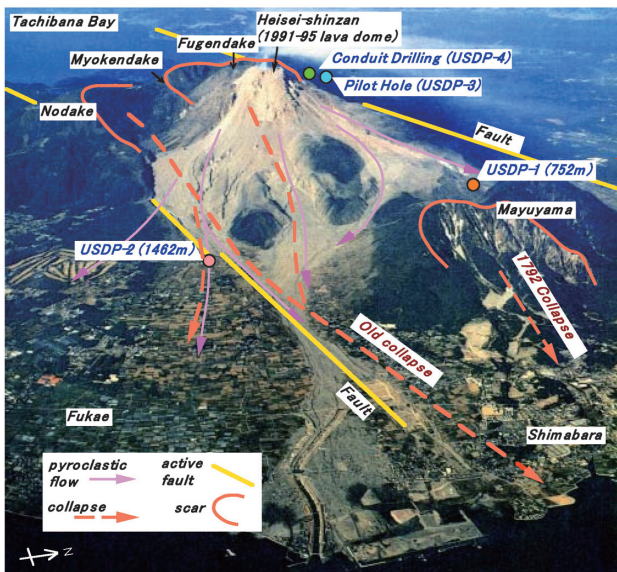


Figure 9. Eastern view of Younger Unzen volcano.

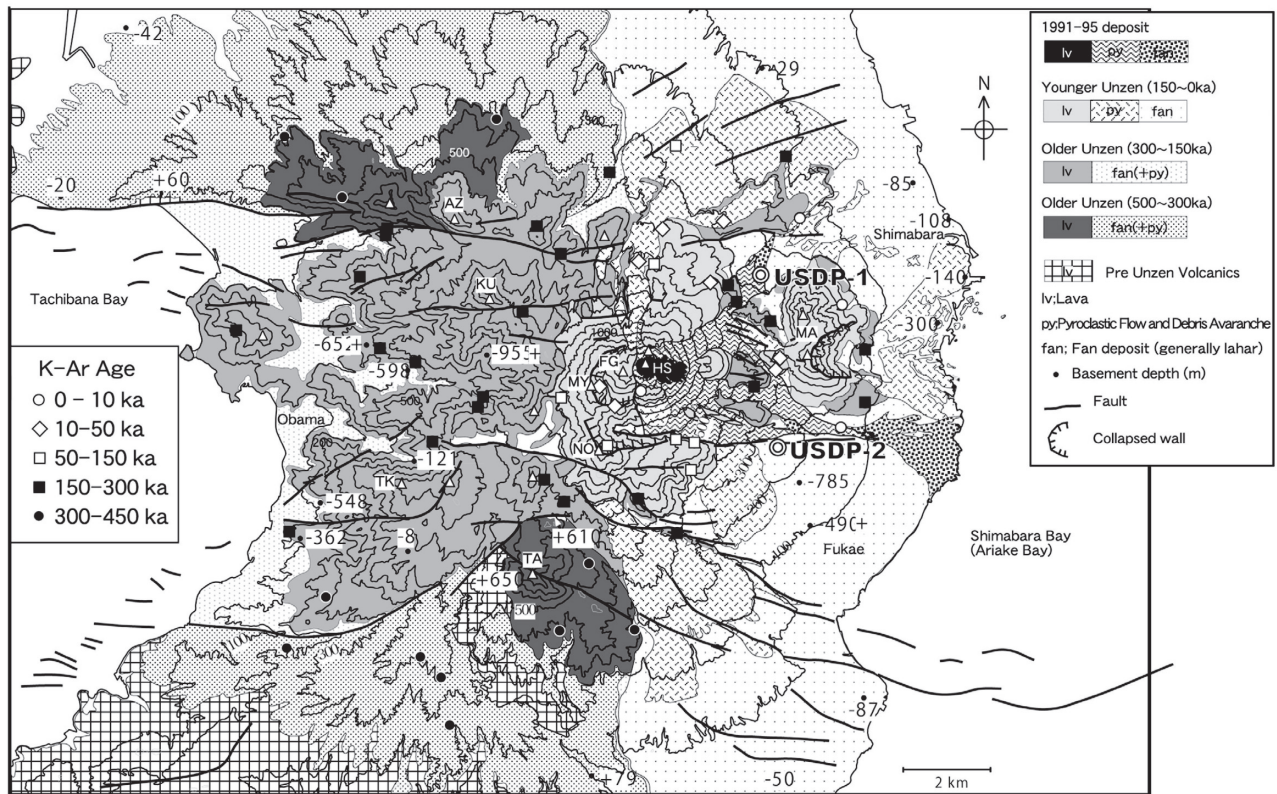
3. Unzen Volcano

A new lava dome (Heisei-Shinzan) growth started since May 20, 1991 that made the 1.2 km long and 0.8 km wide lava dome complex (Fig. 9). More than 9400 Merapi-type pyroclastic flows

(block-and-ash flows) occurred from lava dome collapse during the 1991-95 Unzen eruptions. An ash cloud surge associated with a pyroclastic flow at 16:08 on June 3, 1991 killed 43 people, including Maurice and Katia Krafft and Harry Glicken. The six-year scientific Drilling Project (USDP) revealed a detailed stratigraphy and growth history of Unzen volcano that could penetrate the new 1991-95-conduit system. Mayuyama lava dome that collapsed in 1792 caused a large-volume debris avalanche and tsunami that resulted to 15,000 fatalities. We will focus on the 1991-95 eruptions, disasters and eruptive history of Unzen Volcano in detail.

3-1. Geology and eruptive history

The volcanic products of Unzen volcano cover a wide area, spanning about 20 km E-W and 25 km N-S consisting of multiple lava domes, thick lava flows, and pyroclastic deposits comprised of hornblende andesite and dacite (Fig. 10). The Unzen graben is one of several intra-arc to back-arc rifts that extend en echelon in Kyushu Island, extending west to east for a distance of 20-30 km long. The



AZ=Azumadake; FG=Fugendake; HS=Heisei-Shinzan; KU=Kusenbudake; MA=Mayuyama; MY=Myokendake; NO=Nodake; TA=Takaiwayama; TK=Takadake

Figure 10. Geologic sketch map of Unzen Volcano with K-Ar ages.

northern and southern boundaries of the graben are not clear because volcanic rocks have almost entirely filled the depression.

The Unzen Volcano began to grow at 0.5 Ma and is built on the similarly aged Pre-Unzen pyroxene andesite. Unzen volcanics are characterized by abundant (> 25 vol.%), large (> 3 mm), hornblende and plagioclase phenocrysts that do not vary greatly in composition or appearance throughout most of the eruptive history. The very early products have smaller phenocrysts (2-3 mm) and are transitional from pre-Unzen pyroxene andesites. Unzen Volcano has been divided into three volcanic edifices, Older (0.5-0.3 Ma), Middle (0.3-0.15 Ma) and Younger Unzen (0.15-0 Ma) stages (Fig. 10) according to results from geologic surveys and drillings cores of USDP (Unzen Scientific Drilling Project). The core stratigraphy of the drillings shows the half million years old complete history of Unzen Volcano. Large numbers of block-and-ash flow deposits were found in the Middle Unzen stage (150-300 ka). Explosive pumice flow was found in the Older Unzen stage (300-500 ka). The pre-Unzen basement rocks were

found at the 1200 m depth from the surface at the USDP-2 borehole (Fig. 11). The total eruptive volume of the Unzen Volcano is more than 120 km³.

Older Unzen stage: 0.5-0.3 Ma

Products of Older Unzen comprise volcanic fans extending northwards and southwards from the Unzen graben, and are buried beneath the younger deposits inside the graben. The products consist of deposits of pumice-rich pyroclastic flows, block-and-ash flows, and associated volcanoclastic debris flows. The north-dipping fan spreads outside of the graben and is sharply cut by an E-W trending fault. Inward extensions of these two volcanic fans inside the graben and their sources are inferred to be located far above the skyline of the current summit area of Unzen Volcano.

Middle Unzen stage: 0.3-0.15 Ma

Among the Middle Unzen (0.3-0.15 Ma) volcanic products, lavas that flowed west and east are variable. In the western half of Unzen Volcano, thick lava flows are widespread inside the Unzen graben. Pyroclastic flow and related debris flow

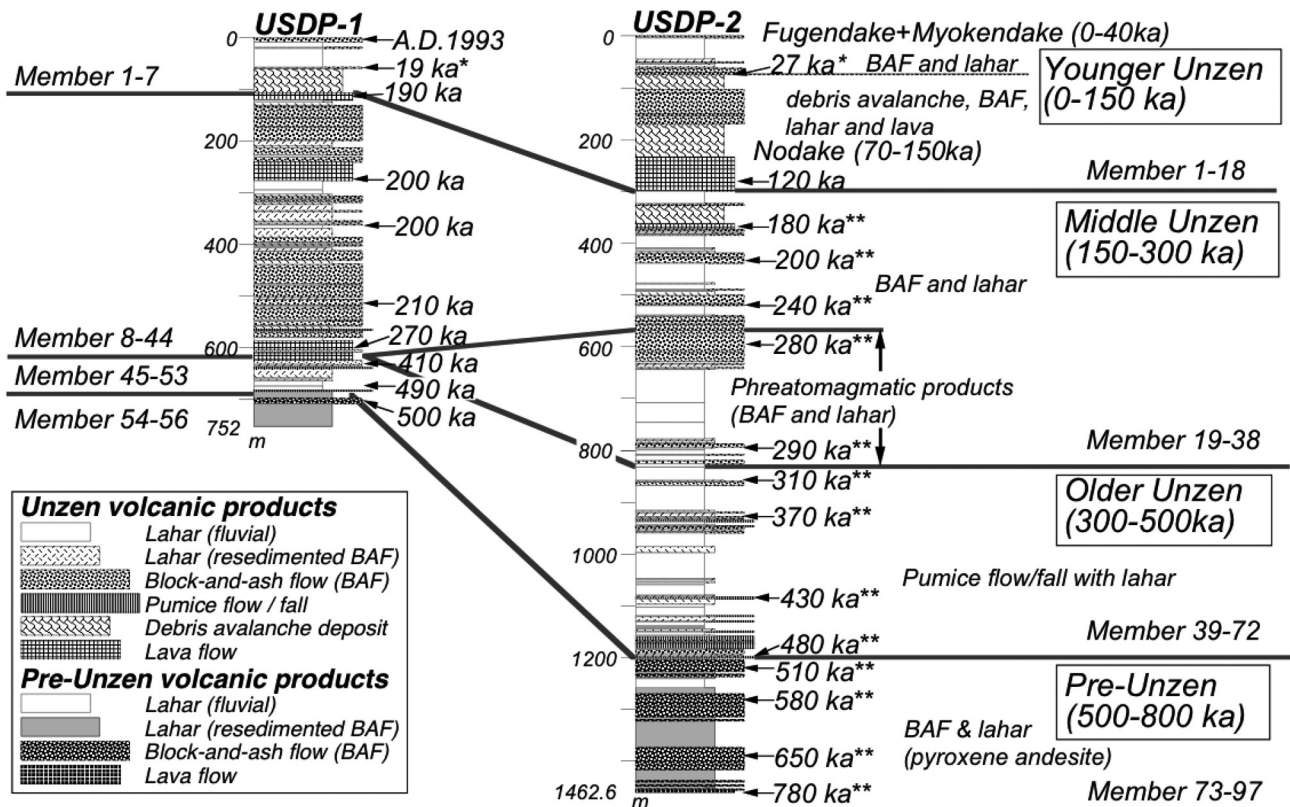


Figure 11. Core stratigraphy of Unzen volcanic rocks along with K-Ar, ⁴⁰Ar/³⁹Ar and ¹⁴C ages. *: ¹⁴C age, **: ⁴⁰Ar/³⁹Ar age.

deposits are almost absent from the surface exposures. Lava flows of 0.2-0.26 Ma are exposed in the eastern half of the volcano as occasional outcrops.

Younger Unzen stage: 0.15-0 Ma

Four volcanic edifices, Nodake, Myokendake, Fugendake and Mayuyama, all located in the eastern half of Unzen Volcano constitute the Younger Unzen stage (Figs. 9, 12). High ridges west of these volcanic edifices acted as topographic barriers, limiting volcanic products from this stage to the eastern half of Unzen Volcano. Continuous subsidence of the Unzen graben without the supply of materials from the vent area to the west resulted in flooding due to inundation of seawater from Chijiwa Bay. Whereas continuous supply of volcanic materials, block-and-ash flow deposits or related debris flow deposits, to the eastern flank of Unzen Volcano exceeded or balanced the subsidence rate of the graben, resulting in continuous development of volcanic fans throughout the history of Younger Unzen Volcano.

Nodake, composed mainly of thick lavas and pyroclastics with debris avalanche deposits, erupted about 70 to 120 ka, and is the oldest volcanic center of the Younger Unzen stage. Myokendake comprises a primary volcanic edifice consisting of pyroclastic deposits. The edifice is little dissected except for an amphitheater, 1.5 km across, and open to the east. Fugendake is developed both inside and outside of the Myokendake Amphitheater. This volcanic center consists of many lava flows, lava domes, pyroclastic flow deposits, and debris avalanche deposits. Located in the easternmost part of Unzen Volcano, Mayuyama comprises two huge lava domes with block-and-ash flow deposits.

Fugendake has been historically active. Eruptions in 1663 and 1792 produced lava flows, and the most recent eruption, in 1991-95 produced lava domes. During the 1792 eruption, the number of earthquakes increased and many cracks were seen on the ground in Shimabara area. An intense earthquake occurred and the Mayuyama edifice collapsed causing a large-volume debris avalanche. This debris avalanche devastated the central area of

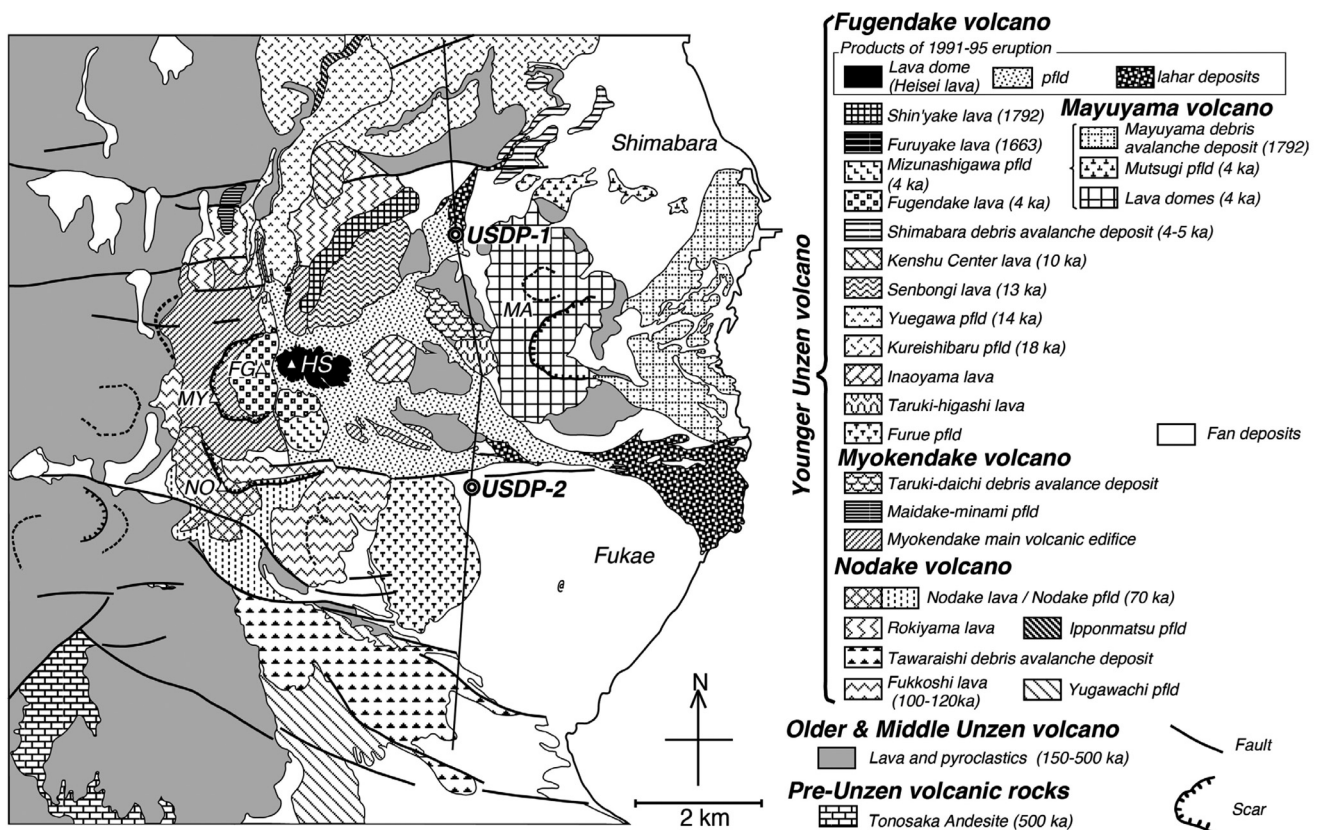


Figure 12. Geologic map of the main part of Younger Unzen volcano (Modified from Watanabe and Hoshizumi, 1995 and Hoshizumi et al., 1999).

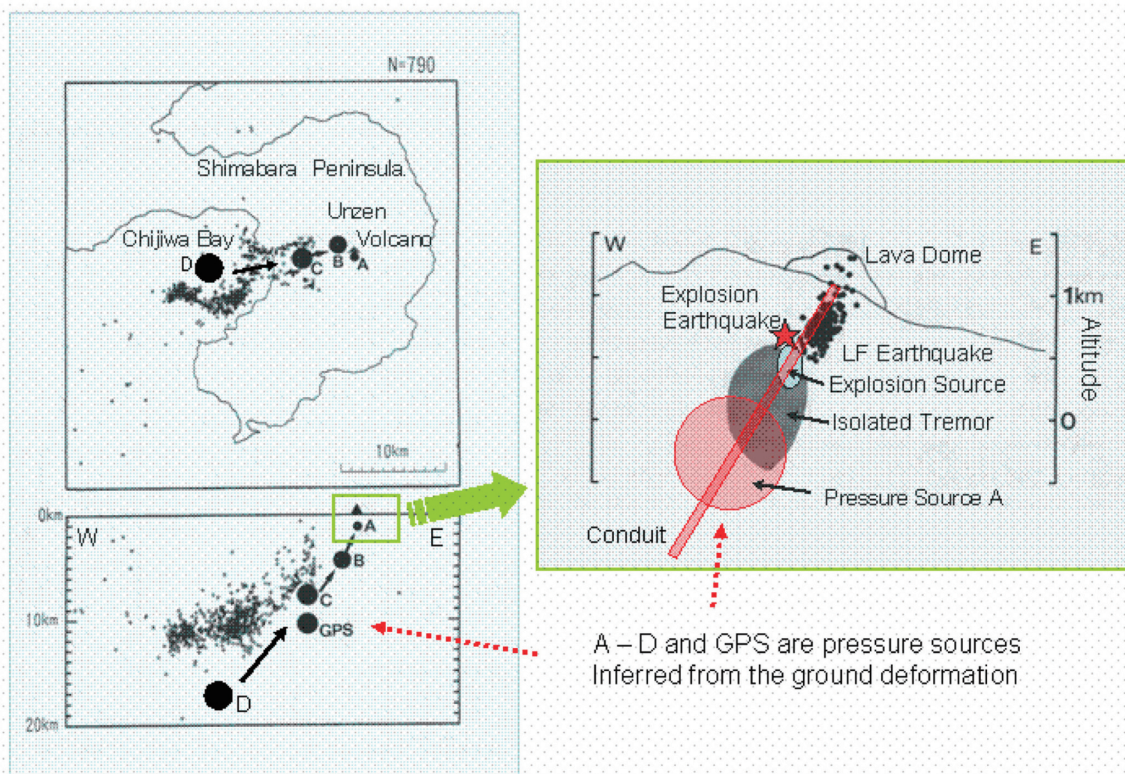


Figure 13. Location of seismic events and pressure sources associated with the 1990-1995 eruption of Unzen Volcano.

Shimabara City before entering the sea to generate a deadly tsunami, which struck the opposite shore of the Shimabara Bay. The events killed about 15,000 people. This was the worst volcanic disaster in Japan.

3-2. Geophysics

Intensive geophysical observations were carried out cooperatively by the national universities and institutes in Japan during and after the 1990-1995 eruption of Unzen Volcano (Shimizu, 1992). These observations provided us information regarding magmatic activity and structure of the volcano.

Magma transport system inferred from seismic activity and ground deformation

Volcano-tectonic earthquakes were very active in the period beginning one year before the eruption and continuing up to the start of the lava dome extrusion. The hypocenters were mostly distributed within a 12 x 20 km area on the western side of the volcano, and shallow eastward toward the summit (Umakoshi *et al.*, 1994; 2001)(Fig. 13, left). A remarkable feature of the hypocenter

distribution is the possibility that it is delineating a ring-fault corresponding to the caldera wall in Chijiwa bay. Another notable feature is alignment of hypocenters in the Shimabara peninsula; the focal area is divided into northern and southern parts by a seismic-gap. Focal mechanism solutions of those earthquakes suggest a pressure source located beneath the seismic-gap. Deflation-inflation sources (sources A-D in Fig. 13) detected by leveling surveys and GPS measurements are situated below an inclined seismic-aseismic boundary (Ishihara, 1993; Kohno *et al.*, 2008; Nishi *et al.*, 1999). These results show that a deep magma reservoir is located at 15-20 km depth beneath the Chijiwa bay, and that the magma ascends obliquely eastward with an inclination of 40-50 degrees.

Magmatic activity in and around the uppermost conduit inferred from geophysical observations

Various seismic- and geodetic-events occurred in the shallow part of volcanic edifice during the 1990-1995 eruption (Shimizu, 1992; Saito *et al.*, 1993; Uhira *et al.*, 1995; Yamasato, 1999; Umakoshi *et al.*, 2002)(Fig. 13, right).

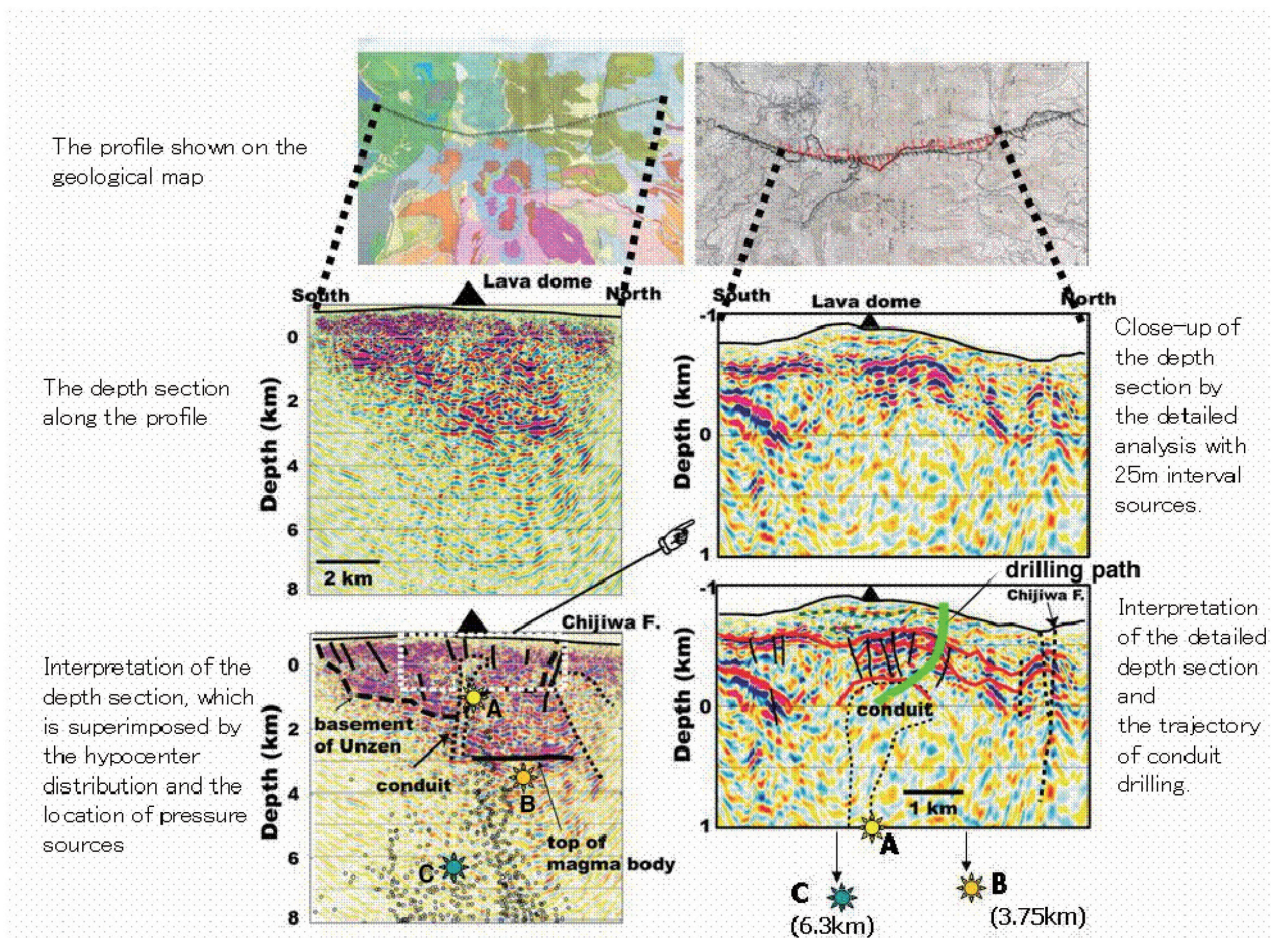


Figure 14. N-S cross section of the subsurface structure of Unzen Volcano deduced from the seismic reflection experiment. The N-S section is along the road on the western flank of Unzen Volcano.

The epicenters of low frequency earthquakes were located in and beneath the growing lava dome at a depth 0-0.5 km below the surface. Sources of the ground deformation associated with vulcanian explosions were located 0.6-0.9 km beneath the crater bottom. The diameter of the pressure sources for these explosions is estimated to be about 40 m. Isolated tremor occurred beneath the summit caldera, whose depth ranged from 0.5 to 2.0 km. The source regions of these events incline westward with a dip angle of about 60 degrees; this suggests that the magma ascended in an oblique conduit. On the other hand, the high frequency earthquakes and ground deformation just before the lava dome appearance can be interpreted by a combination of upward growth of a magma column and lateral intrusion of a dike (Yamashina and Shimizu, 1999). The horizontal extent of the dike exceeded 400 m, and the thickness finally reached about 13 m. The top of the dike was estimated to be about 130 m deep,

although the bottom has not been fully constrained. The diameter of the magma column is obtained as 40 m, consistent with that of the explosion sources. Seismic tomography shows that a low velocity region exists at sea level beneath the summit caldera (Nishi, 2002). The region extends about 1 km in both horizontal and vertical directions, which corresponds both with the source region of isolated tremor and with a high conductivity zone (Kagiyama *et al.*, 1999). This low- V_p region probably represents the extent of the hydrothermal system sustained around the conduit (Hashimoto, 1997).

The seismic reflection experiment

In order to reveal the subsurface structure of Unzen Volcano and to detect the volcanic conduit, a seismic reflection experiment was conducted using vibratory energy sources (VIBROSEIS) in December 2001 as a program of the Unzen

Scientific Drilling Project (Shimizu *et al.*, 2002). About 580 receivers, each consisting of 9 geophones, were deployed at intervals of 25 m along a N-S survey line on the western flank of the volcano. The survey line crosses the Unzen graben and the magma ascent path inferred from geophysical observations. In the experiment, three VIBROSEIS vehicles vibrated at about 280 source points on the survey line at intervals of 25-100 m. Because the source energy of the VIBROSEIS is not enough to penetrate the volcanic edifice, 3-100 sweeps of the vibration signals were stacked to improve the S/N ratio of the data.

The reflection analysis revealed the distribution of structural discontinuities in the N-S cross section of the volcano (Fig. 14). The depression structure of the Unzen graben is clearly recognized in the cross section. The strong reflection at a depth of 3 km is consistent with the location of the pressure source B inferred from geodetic measurements, which probably corresponds to the upper boundary of a magma reservoir. On the other hand, the narrow area, in which the strength of reflection is extremely weak, extends almost vertically from sea level down to the pressure source B. Volcanic earthquakes occur along a narrow area. Thus the area is interpreted as the volcanic conduit or dike intrusion below the western flank of Unzen Volcano.

3-3. Eruption and disaster of the 1990-95 Unzen Eruption

Unzen eruption and lava dome growth

The chronology of the latest eruption was summarized in Nakada and Fujii (1993) and Nakada *et al.* (1999). After 198 years of dormancy, the Unzen Volcano erupted on November 17, 1990. Phreatic eruption started in both the Jigokuato and Kujukushima craters. Preceding this eruption, earthquake swarms occurred in November 1989, and the hypocenters migrated toward the summit. The number of isolated tremor events increased in



Figure 15. Lava dome complex seen from the north. The exogenous part is hanging over the eastern slope of Mount Unzen and the endogenous part has a steaming spine on the flat top.

late-January 1991. Relatively strong phreatomagmatic eruption started in Byobuiwa crater in February, and the activity increased with time. The eruption suddenly stopped on May 12 and intense swelling and strong demagnetization of the crater area began. A lava spine like an onion head protruded within the Jigokuato crater on May 20, 1991 by which time the crater had been widened due to repeated eruption. The spine was broken into several large blocks with flat surfaces. The Jigokuato crater was soon filled with lava blocks, such that older lava blocks were pushed away by new lavas extruded in the center. Collapse of the lava dome started on May 23 and the first pyroclastic flow was witnessed on the morning of May 24.

The lava dome complex that was formed in the last eruption is 1.2 km long (E-W), 0.8 km wide and 0.45-0.25 km thick, and the volume is about 100 million m³ (about half of the total volume of erupted lavas; 210 million m³ as DRE) (Fig. 15). The eastern half of the dome complex that drape the eastern slope of Mt. Unzen predominantly experience exogenous growth, while the western part covered by lava blocks with a relatively flat top is the part that has grown endogenously.

The lava dome grew almost continuously throughout the eruption and is separated into two periods of 20 months (from May 191 to Dec. 1992) and 25 months (from Feb. 1993 to Feb. 1995) with different supply rates, where the maximum effusion rate was about $400,000 \text{ m}^3/\text{d}$ ($5 \text{ m}^3/\text{s}$) in September 1991. Initial growth of the lava dome over the eastern edge of the Jigokuato Crater (Fig. 16) was unstable, resulting in the partial collapse of the moving front of the lava dome. The dome increased its dimension with time. It grew mainly exogenously when the effusion rate was high, and endogenously when the effusion rate was low. The exogenous part was made up of 13 discrete lava lobes, most of which had been active for several months. Typical dimensions of the individual lobes are 300-400 m long, 200-300 m wide and 50-100 m thick, except for lobe 11 with the largest dimension. The moving speed of lava was up to 50m/d near the vent, and decreased toward the lobe front, where the lava was cooled during flow. After lobes reached over 350 to 400 m in length from the vent, new lobes started growing within the spaces near the vent not occupied by previously lobes. The birth of new lobes was clearly detected by elevated activity of near-surface low-frequency earthquakes. During exogenous dome growth, deformation of the crater floor was minor, while it was substantial during endogenous growth. By the beginning of the main

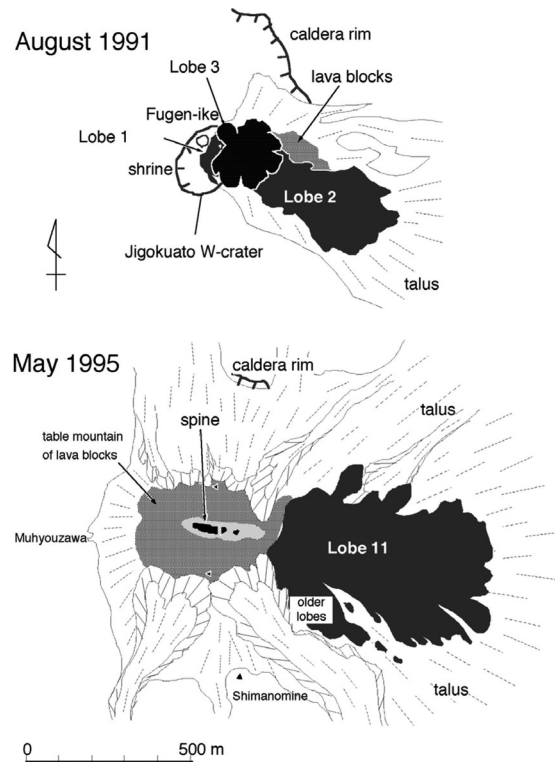


Figure 16. Schematic sketches showing different periods of the lava dome complex of Mount Unzen (Nakada *et al.*, 1999).

endogenous growth event in late November 1993, the eastern half of the dome complex had been occupied by piles of lava lobes up to 200-300 m thick. The growth of the endogenous dome was proposed by Nakada *et al.* (1995) to be similar to that of pillow lava or pahoehoe lobes. Growth of lava dome was ended with intrusion of a spine into

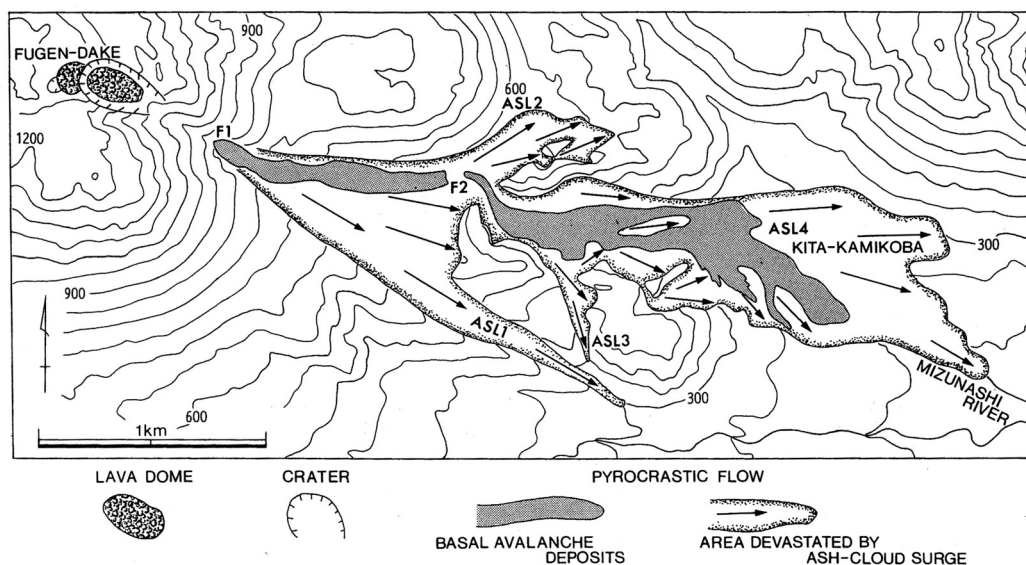


Figure 17. Distribution of the June 3, 1991 pyroclastic flow deposit (Yamamoto *et al.*, 1993). Arrows are the flow direction of the ash-cloud surge as indicated by blown-down trees. F1 and F2 indicate steep slopes along the Mizunashi River. ASL, ash-cloud surge lobe.

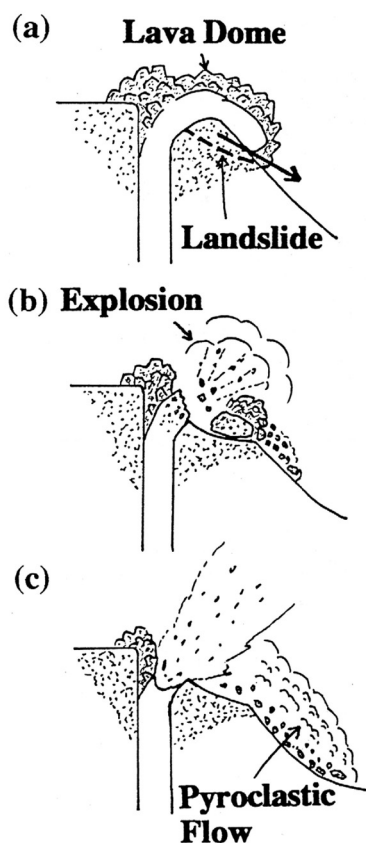


Figure 18. Initiation mechanism of pyroclastic flow on June 8, 1991 (Takarada *et al.*, 1993a). (a) landslide triggered the collapse of lava dome, (b) explosion due to sudden pressure reduction, (c) pyroclastic flow generated by broken up materials of the lava dome and basement.

the center of the endogenous portion, just above the crater (Jigokuato Crater) where lava first appeared in May 1991 (Fig. 16). The spine started its growth in October 1994, and was associated with relatively strong swarms of earthquakes within the dome above the Jigokuato Crater. The dimension of the spine is about 40 m wide by 100 m long.

After the end of dome growth (February 1995), the dome complex began shrinking slowly at a constant rate. The deformation has continued as of 2007. Fumarolic activity started from the foot of the spine soon after its birth reaching temperatures up to 300 °C in mid 2007. The temperature dropped to 250 °C in 2007 and 90 °C in 2011.

Pyroclastic flows

More than 9400 Merapi-type pyroclastic flows (block-and-ash flows) occurred from lava dome collapse at Unzen Volcano during the 1990-95 eruption. A new lava dome (Heisei-Shinzan) formed at the Jigokuato crater on May 20, 1991. The dome continued to grow on May 23 and juvenile blocks began falling from its margins down the steep eastern slopes. On May 24, a reddish-brown ash-laden plume was observed above the eastern flank of Fugendake as a portion of the lava dome

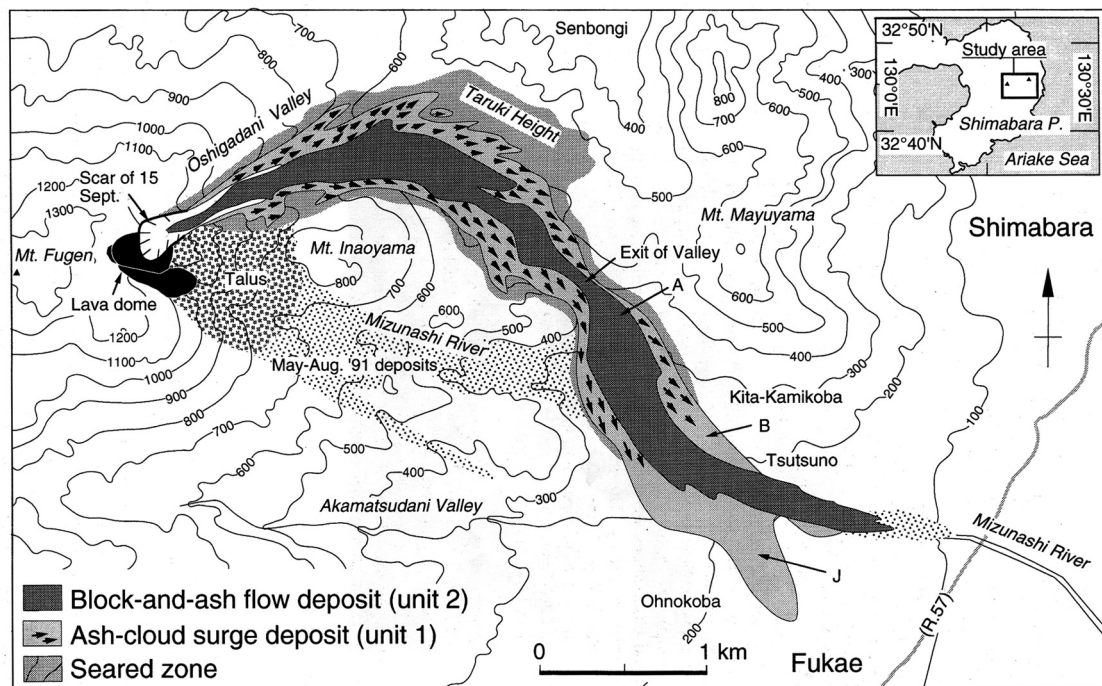


Figure 19. Distribution of the Sep. 15, 1991 pyroclastic flow deposit (Fujii and Nakada, 1999). Arrows in ash-cloud surge deposit represent the current direction as indicated by toppled trees. 'A' and 'B' indicate observation points, where several people were killed by ash-cloud surge on June 3, 1991, 'J' indicates the site of Onokoba elementary school.

collapsed, producing the first pyroclastic flow that traveled about 1 km down the flank. Growth and collapse of the new lava dome continued, generating pyroclastic flows from collapse events. Major pyroclastic flows, including those on June 3 and 8, September 15, 1991, and June 23 and 24, 1993, occurred during exogenous growth when the effusion rate was very high (Nakada and Fujii, 1993). Descent paths of pyroclastic flows were controlled by the growth direction of the lava dome.

A series of pyroclastic flows descended the Mizunashi River at 16:08 on June 3, 1991 (Fig. 17). The runout distance was about 3 km and the volume of this event was about 0.5 million m³ in DRE (Nakada *et al.*, 1999). An ash-cloud surge associated with the pyroclastic flow killed 43 people, including Maurice and Katia Krafft and Harry Glicken in Kita-Kamikoba area. Co-ignimbrite ash fall was distributed more than 100 km away from Shimabara (Watanabe *et al.*, 1999). In all, 147 houses were burned or destroyed.

An explosive pyroclastic flow event was coeval with a vulcanian explosion. Estimated speeds of the early stage pyroclastic flows were up to 150 km/h (Takarada *et al.*, 1993b). On June 8, a landslide including the basement of the lava dome occurred that caused a sudden pressure reduction in the lava dome and conduit, resulting in explosive eruptions (Fig. 18). The pyroclastic flows descended 5.5 km and had a flow volume of 0.7 million m³ (Nakada *et al.*, 1999). In all, 175 houses were burned or destroyed. On June 11, a similar explosive event occurred, but no large-scale pyroclastic flows were observed.



Figure 20. 5:25 June 24, 1993 pyroclastic flow descending toward the Senbongi area at the NE foot of the Unzen Volcano (Photo taken by Setsuya Nakada).

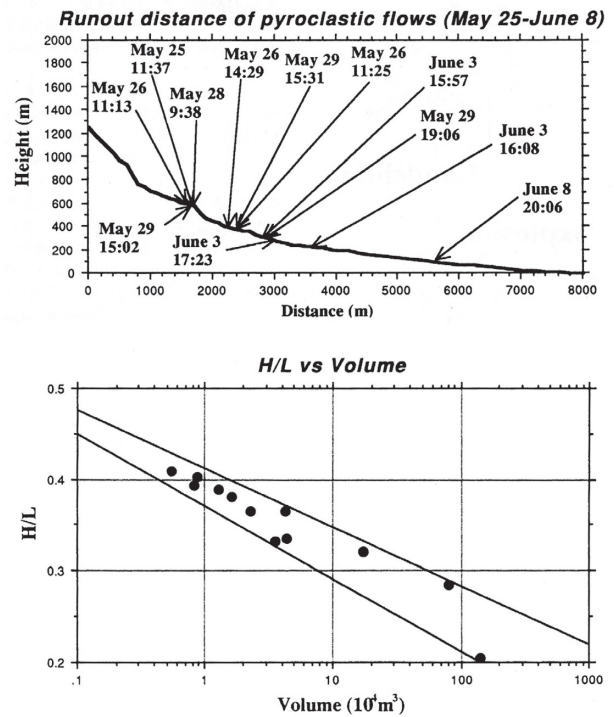


Figure 21. Relation between the volume and H/L (height vs runout distance) ratio of pyroclastic flows (Takarada *et al.*, 1993a). Large-volume pyroclastic flows have lower H/L ratio (high mobility) than the small-volume pyroclastic flows.

The largest pyroclastic flows occurred on September 15, 1991, caused by a large-scale collapse of the northern part of the dome complex. Multiple pyroclastic flows starting at 16:44 and successively at 17:59, 18:42, and 18:54 cascaded down the Oshigadani Valley (Fig. 19). Estimated speed of the first flow was 200 km/h (Miyahara *et al.*, 1992). Their flows descended along the Oshigadani Valley and reached the Mizunashi River, following the topographic low. However, pyroclastic surges rushed straight from the exit of the Oshigadani Valley and damaged the Onokoba Elementary School. In all, 218 houses and buildings including the Onokoba Elementary School were burned or destroyed. The runout distance of the pyroclastic flows was about 5.5 km. The volume of the largest flow was ~ 1 million m³, while the total volume of this event was about 2.4 million m³ (Fujii and Nakada, 1999).

On June 23 and 24, 1993, a series of pyroclastic flows descended the Nakao River. Pyroclastic flows starting at 2:52 and successively at 11:14 on June 23, and 5:25 on June 24, 1993, cascaded down the gorge in the Nakao River (Fig. 20). One person who

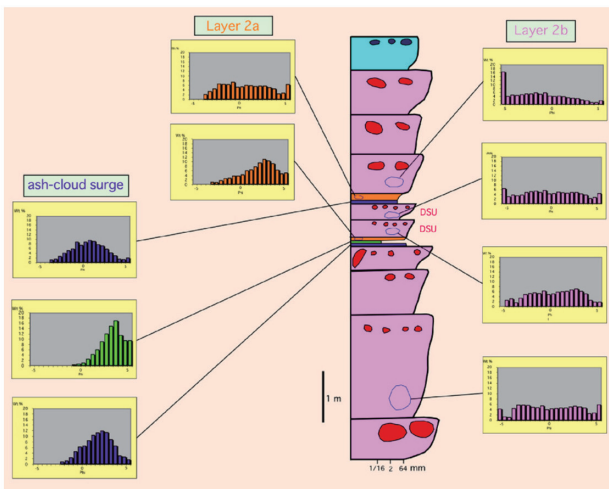


Figure 22. Columnar section and grain-size distributions of block-and-ash flow and ash-cloud surge deposits in the Oshigadani Valley.

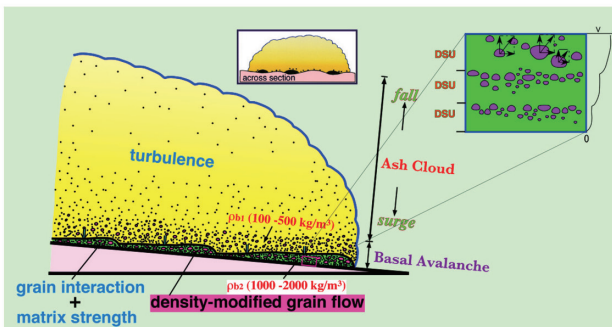


Figure 23. Transport and depositional model of the 1991-95 Unzen pyroclastic flow (Takarada and Melendez, 2006).

entered in the evacuation area was killed by a pyroclastic surge associated by the second flow. In all, 211 houses were burned or destroyed. The runout distance was about 4 km and the volume of each flow was approximately 0.5 million m³. The total volume of this event reached about 2.1 million m³. In total, 800 houses were burned by pyroclastic flows/surges during the 1991-95 Unzen eruption (Ohta, 1997).

The volume of each pyroclastic flow was estimated using seismic tremor records (Takarada *et al.*, 1993a). Large-volume pyroclastic flows have relatively low-H/L (height vs runout distance) ratio (high mobility) compared to small-volume pyroclastic flows (Fig. 21).

The pyroclastic deposits comprise > 10 flow units (Miyabuchi, 1999). Lobes (< 10 m wide) and levees (< 2.5 m wide) were sometimes developed on the depositional surface. The thickness of a flow unit ranges from 0.2–2 m. Each flow unit contains <

2 m size, reversely graded, sub-angular to sub-rounded blocks. The flow units occasionally display several 10-25 cm thick, reversely graded depositional subunits (DSU) (Fig. 22). Clasts (5-20 cm) are aligned at the top of each DSU. The layer 2a (Sparks *et al.*, 1973; < 20 cm thick, <5 cm size clasts) unit usually occurs at the base of the flow unit. Massive to laminated ash-cloud surge beds (< 20 cm thick) are observed infrequently between flow units. Ash-cloud surge beds lack the coarser and finer fractions that are often observed in pyroclastic flow deposits. The large reversely graded, sub-angular to sub-rounded blocks and basal layer 2a suggest that interactions between blocks occurred during the depositional stage. Night video image taken by the Self Defense Force shows large blocks rolling and saltating suggesting turbulent transport of pyroclastic flows (Fig. 23). Large blocks accumulate at the bottom of turbulent flow

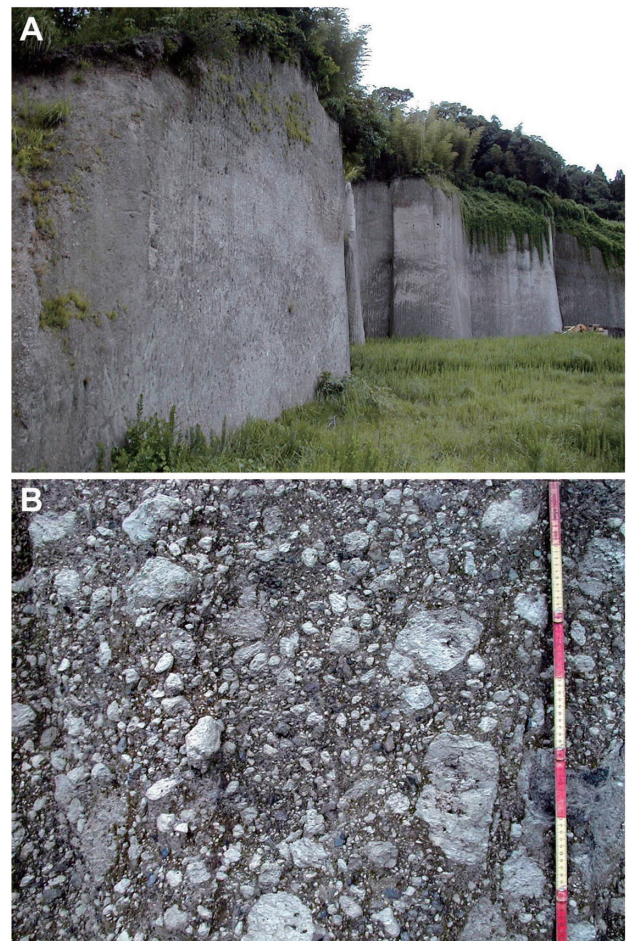


Figure 24. The Oyatsu sub-unit of the Aso-4 pyroclastic flow deposits. (A) Non-welded pumice flow deposit at Stop 1-1. (B) Abundant pumice clasts in the Aso-4 pyroclastic flow deposit (Oyatsu sub-unit). Scale segments are 10 cm.

due to variations in slope angle and channel width. Slow-speed lobate high-density grain flows developed at the base of a relatively high-speed turbulent pyroclastic flow. The 5-25 cm thick DSUs in the flow units suggest that blocks and matrix forming basal lobate grain flows accumulated through successive aggradation. The basal grain flows ceased when the shear stress in the flow became lower than the yield strength of the matrix.

4. Guide to the stops

4-1. Day 1: Aso caldera and the related pyroclastic-flow deposits

The original fieldtrip group starts in the morning at downtown of Kumamoto City and travels to Aso Volcano by chartered bus.

Stop 1-1: Mashiki (ca. 10 km SW of Aso caldera) Aso-4 pyroclastic flow deposit

The Aso-4 pyroclastic flow deposit (hornblende dacite) is the uppermost and most voluminous pyroclastic deposit of the Aso pyroclastic flow deposits. It covered much of central Kyushu (Fig. 3). The deposit is composed of two units (Aso-4A and Aso-4B in ascending order) in the eastern region of Aso Volcano (Ono *et al.*, 1977). In contrast, the Aso-4 pyroclastic flow deposit is divided into eight sub-units in areas at the west of Aso caldera (Watanabe, 1978). Each sub-unit can be identified by lithological features such as color, grain size, texture, degree of welding and mineral composition. The Oyatsu white pumice-flow deposit is the lowermost sub-unit of the Aso-4 pyroclastic flow deposits. At Stop 1-1, the Oyatsu pyroclastic flow deposit is more than 10 m thick, non-welded and contains abundant well-vesiculated pumice in an ash matrix with andesitic and metamorphic fragments (Fig. 24).

Stop 1-2: Namino (near the eastern caldera rim) Holocene fallout tephra from post-caldera central cones

A thick tephra sequence erupted from the post-caldera central cones is preserved above the Aso pyroclastic-flow plateau, especially in the east of the caldera, because tephra dispersal is affected by the prevailing west to southwest wind direction in Japan. The total thickness of fallout tephra

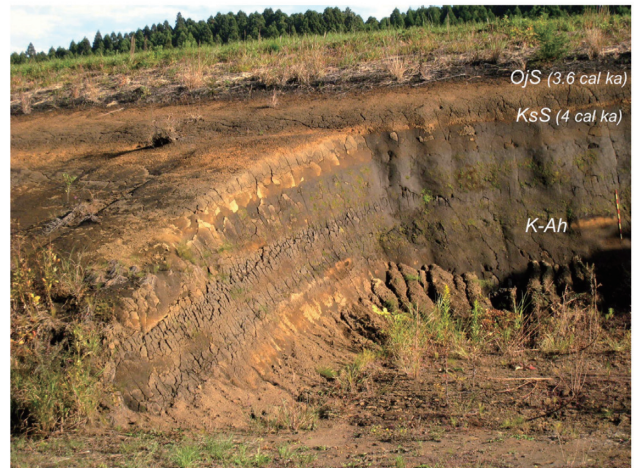


Figure 25. Holocene post-caldera fallout tephra section at Namino, east of Aso caldera.

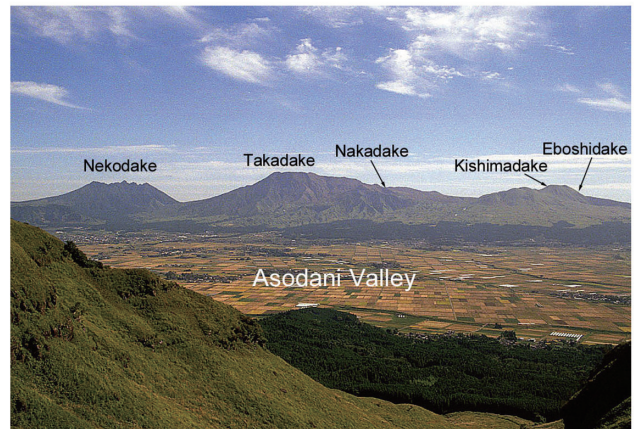


Figure 26. View of post-caldera central cones of Aso Volcano from Daikanbo lookout.

deposits after the Aso-4 eruption reaches about 100 m at the eastern caldera rim. We will observe a tephra section located near the eastern rim of Aso caldera. The section presents outline of Holocene tephrostratigraphy of Aso Volcano. Fallout tephra layers from post-caldera central cones are interbedded between black humic soil layers (Fig. 25). Marker Holocene tephra including Ojodake scoria (OJS; 3.6 ka) and Kishimadake scoria (KsS; 4 ka) are clearly identified at the section. Although the sequence is composed mainly of minor fallout tephra deposits from post-caldera central cones of Aso Volcano, a widespread tephra from another volcano is intercalated in the sequence. The widespread tephra is orange Kikai Akahoya ash (K-Ah; Machida and Arai, 1983, 2003), which is co-ignimbrite ash-fall deposit produced by the 7.3 ka catastrophic eruption at Kikai caldera (southern



Figure 27. Lag breccia of Aso-4 ignimbrite at Kario, northwestern rim of Aso caldera.

Kyushu; ca. 300 km south of Aso Volcano). K-Ah tephra includes abundant bubble-wall glass shards, and is very useful for correlation of tephra sequence not only at Aso Volcano but also in most part of Japan.

Stop 1-3: Daikanbo lookout

Overlook of Aso caldera and post-caldera central cones

Daikanbo lookout, 936 m in elevation, is located on the top of the northern rim of Aso caldera. The overlook provides an excellent view of geomorphic features of Aso caldera and post-caldera central cones aligned in an E-W direction. The size of the caldera is 25 km north-south and 18 km east-west and the relative height of the caldera wall is about 400 m at Daikanbo. This large caldera has been formed by four explosive eruptions from 270,000 to 90,000 years ago. Flattened slopes



Figure 28. Aerial view of Nakadake showing geomorphic structure of the volcanic edifices. CL: craterlet.

radiating outward from the caldera rim are formed by deposition of gigantic pyroclastic flow deposits. Five peaks can be distinctly seen from the lookout. They have been called Aso Gogaku (five peaks of Aso mountains: Nekodake, Takadake, Nakadake, Kishimadake, Eboshidake from east to west). The shape of the five mountains has been said to resemble a reclining Buddha (Fig. 26). Nekodake, the easternmost, is a dissected stratovolcano formed in the period between Aso-2 and Aso-3 eruptions, though it looks like a member of the post-caldera central cones. From the lookout, we can see Kuju volcano to the northeast, a complex of dacite to andesite lava domes with basal areas of pyroclastic flow deposits. Restroom facilities are available.

Stop1-4: Kario (northwestern caldera rim)

Lag breccia of Aso-4 pyroclastic flow deposit

After leaving Daikanbo lookout, we will arrive at the Kario section. The Aso-4T pyroclastic flow (the Tosu orange pumice-flow; Watanabe, 1978) deposit, one of the upper subunit of the Aso-4 flows, is a low-aspect-ratio ignimbrite (Suzuki-Kamata and Kamata, 1990). The lag breccia of the Aso-4T pyroclastic flow deposits overlain by ash flow deposit can be observed at the section. It is more than 2 m thick and contains a large amount of accidental lithic fragments with few amount of orange pumice (Fig. 27). The breccia is dominated by andesitic rocks, but gabbro and diorite derived from Cretaceous basement rocks of Aso caldera are recognized.

4-2. Day 2: Geology of post-caldera central cones of Aso volcano

Most of the second day will be used to see post-caldera central cones of Aso Volcano. We will leave Aso around noon and go to Unzen by bus and ferry boat.

Stop 2-1: Nakadake crater

CAUTION: This crater area is very dangerous. Persons having bronchial diseases should take special care. Nakadake crater always emits volcanic gas including SO₂ and the gas concentrates in the topographic lows.

Nakadake, the only active central cone of Aso Volcano, is a basaltic andesite to basalt



Figure 29. Photographs of Nakadake crater. (A) 1st crater showing a hot water pool. (B) 4th crater and its crater wall composed of thick agglutinate (ca. 20 m).

stratovolcano composed of the old edifice, the young edifice and the youngest pyroclastic cone (Fig. 28). The western half of the upper part of the old edifice was destroyed by a northwestward-directed collapse, leaving a 250 m-high collapsed wall (Ono *et al.*, 1995). The active



Figure 30. Aerial view of Kusasenrigahama crater and Eboshidake Volcano.

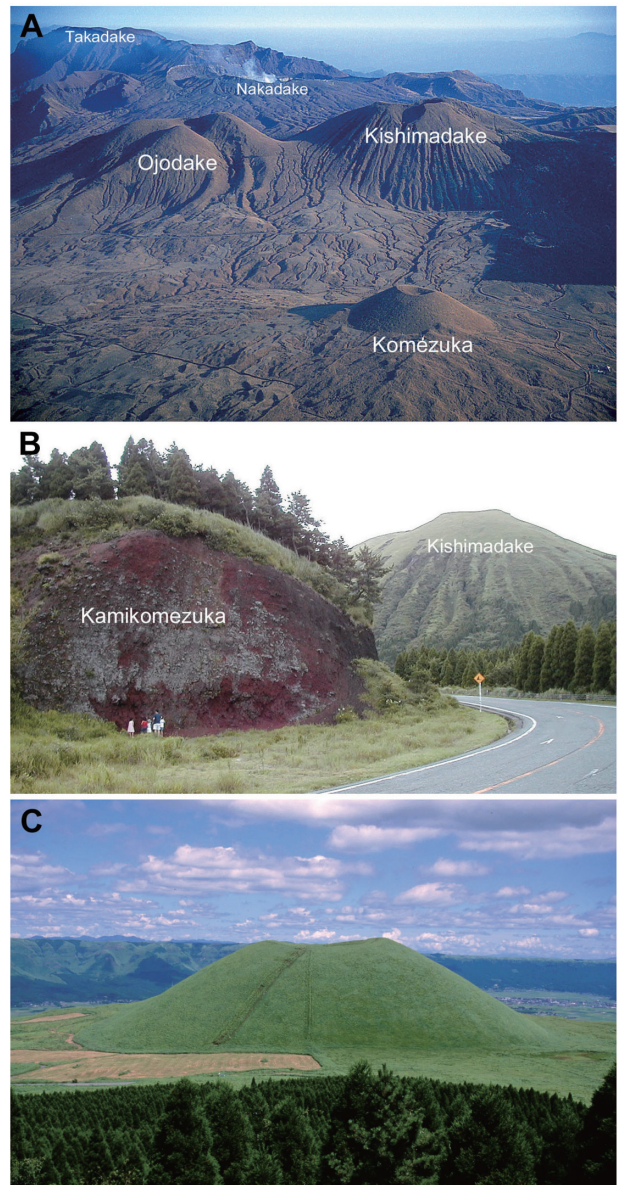


Figure 31. Holocene scoria cones of Aso Volcano. (A) Aerial view of Holocene scoria cones from the northwest. (B) Cross section of the Kamikomezuka scoria cone. (C) Northern view of Komezuka scoria cone.

crater of Nakadake, formed in the youngest pyroclastic cone, is a composite of seven craterlets aligned N-S. The northernmost (1st crater) is the only one that has been active during the past 70 years. During dormant periods a blue or green colored hot water pool stays at the bottom of the 1st crater (Fig. 29A). Other craterlets were active before 1933 AD. The wall of the southernmost craterlet (4th crater) is mainly composed of a densely welded agglutinate formed during a prehistoric eruption (Fig. 29B).

The summit crater of Nakadake is accessible by a toll road and a cable car, and a large number of

tourists visit there all year round. The SO₂ concentration of volcanic gas has been monitored automatically since 1998. Entering the crater area is prohibited when the monitored concentration of volcanic gas is high. If the gas condition permits, we can visit the crater area and walk the loop trail along the craterlets. Restroom facilities are available.

Stop 2-2: Kusasenrigahama crater

Kusasenrigahama crater is a 1 km-diameter crater on the northern flank of Eboshidake Volcano (Fig. 30). One of the largest plinian eruptions occurred here about 30 ka (calibrated ¹⁴C age; Miyabuchi, 2009). The eruption emplaced pumice fall deposits around Aso caldera and formed densely welded pumice layers near the crater (Ono and Watanabe, 1985). The dense rocks of welded pumice can be observed on the surface adjacent to the southern wall of the crater. At present the crater is beautiful grassland with ponds and we can enjoy horse-riding in the crater.

Aso Volcano Museum is in front of the

Kusasenrigahama crater. The museum introduces Aso Volcano using wide-screen movies, video and many interpretative displays. Restroom facilities and souvenir shops are available in the Museum.

Stop 2-3: Kamikomezuka scoria cone

CAUTION: Be careful of traffic and falling rocks.

Several scoria cones were formed on the northwestern slopes of central cones in Holocene time (Fig. 31A). This stop provides an opportunity to see a cross section of a scoria cone. The vent is probably located at the left side and poorly-sorted scoria fall deposits are crudely stratified (Fig. 31B).

The stop also provides a good view of Komezuka scoria cone (Fig. 31C). The scene of Komezuka is one of the most representative views of Aso Volcano. The beautiful shape of the cone looks like an overturned bowl.

Way to Shimabara

After leaving the Kamikomezuka scoria cone, we will go to Shimabara at the eastern foot of Unzen

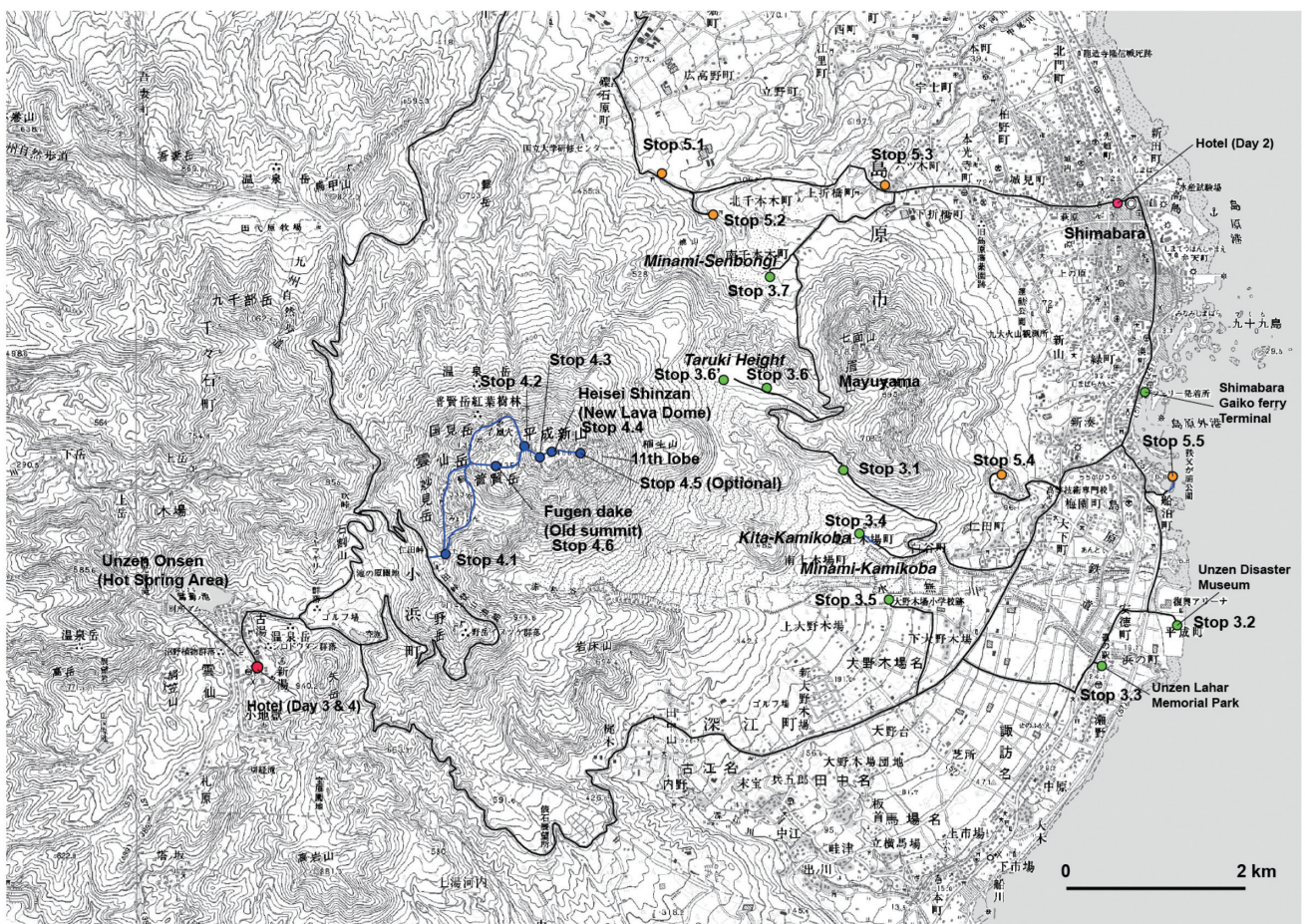


Figure 32. Locality points showing on a 1:50,000 topographic map of Unzen volcanic area.



Figure 33. Eastern view of the Heisei-Shinzan New lava dome.

Volcano, via Kumamoto city through highway 57. About one and half hour drive will take us to Kumamoto port and we will board a ferryboat to Shimabara. A one hour cruise across the Ariake Sea will take us to the eastern base of Unzen Volcano. Before arriving at Shimabara city, the ferry boat provides a panoramic overview of Unzen Volcano: the 1991-1995 lava dome and apron of pyroclastic flow deposits appear in the background, the 1792 debris avalanche scar of Mayuyama Volcano appears on the right of the Unzen dome and the

debris-avalanche deposit forms hummocky hills in the Ariake Sea.

4-3. Day 3: The 1991-95 Unzen pyroclastic flows

On Day 3 we will mainly focus on the 1991-95 Unzen pyroclastic flow deposits in detail. Localities are shown in Fig. 32.

Stop 3-1: Southern flank of Mayuyama. Lookout point of the Heisei-Shinzan and the Unzen pyroclastic flow deposits

This is the first lookout point for the new lava dome (Heisei-Shinzan) and the thick pyroclastic flow deposits (Fig. 33). We will climb to the top of the new lava dome the next day. The 11th lobe of the lava dome is seen in front of us. In all, more than 9400 pyroclastic flows occurred due to the collapse of unstable portions of the lava dome from May 24, 1991 to 1995. The Kita-Kamikoba area that we can look down to is the site where 43 people were killed by the June 3 pyroclastic surge, including Maurice and Katia Kraft and Harry Glicken. We will visit this area at stop 3-4. The Sep. 15, 1991 pyroclastic flow descended the Oshigadani valley (in front of us) and the ash-cloud surge reached the Onokoba Elementary School.

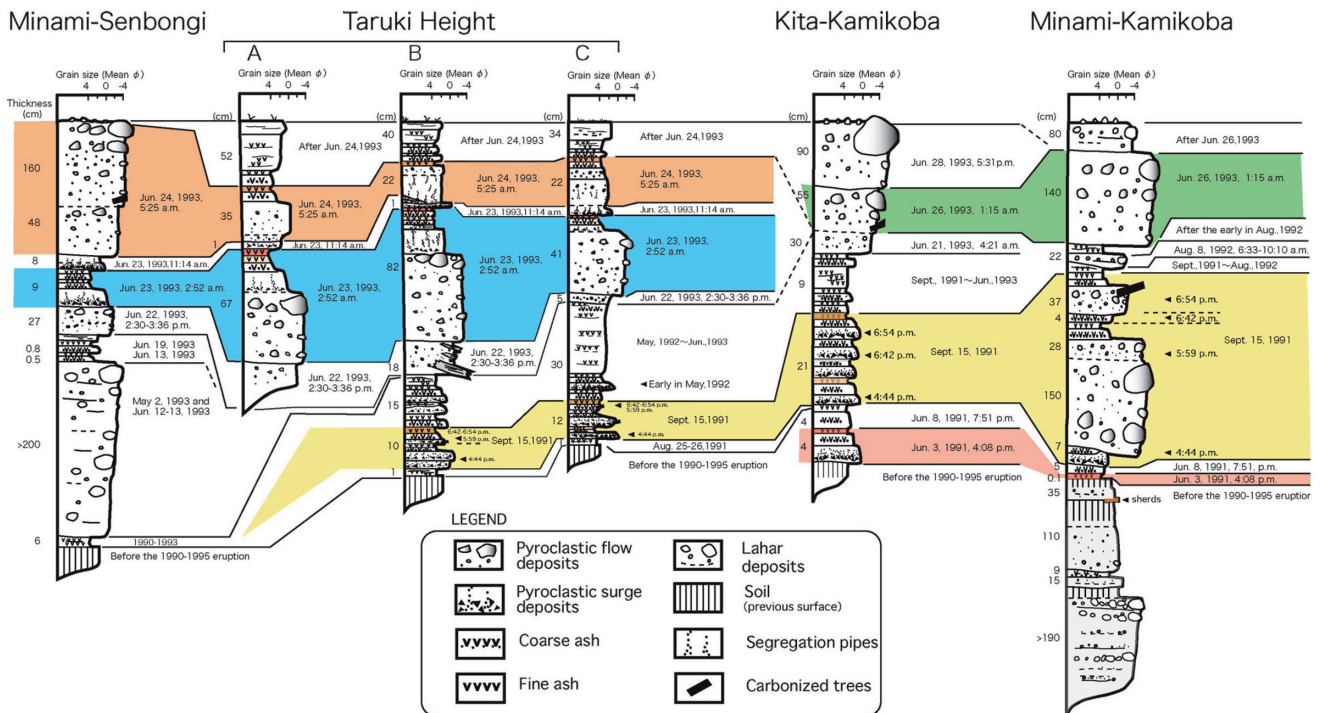


Figure 34. Stratigraphic columns of the 1990-95 eruptive products at NE to SE flank, Unzen Volcano

Shimanomine lava dome (4-6 ka) is seen at the left of the new lava dome. Myokendake Amphitheater is located at the backside of these domes (Fig. 12). The collapse that caused a large-scale debris avalanche at 20-30 ka formed the Myokendake Amphitheater. Tarukidaichi debris avalanche deposit on the Tarukidaichi may correspond to this stage. Nodake Volcano (70-120 ka) is seen at the left of Shimanomine lava dome. The Nodake Volcano produced Tawaraishi debris avalanche and Yugawachi pyroclastic flow deposits, which is seen at the south side. E-W trending Akamatsudani and Fukae normal faults are seen at the south side. The Unzen volcanic area is developed in the active graben system. The depression rate is 2mm/year. Inaoyama lava dome (undated), Iwagamiyama and Kadowakiyama lava domes (Older Unzen stage, 0.5-0.3 Ma) are seen in front. Taruki-Higashi lava dome (30-20 ka) is seen at the north. The Mayuyama lava dome (4-5 ka) is seen at the backside (northern side). The Mayuyama lava dome is composed of northern Shichimenzan and southern Tenguyama lava domes. Bottom of the Tenguyama lava dome is composed of block-and-ash flow deposits. We are looking western slope of the Tenguyama lava dome. The other side of the Tenguyama lava dome was collapsed and produced the Mayuyama debris avalanche on May 21, 1792.

Stop 3-2: Unzen Disaster Museum

Unzen Disaster Museum provides comprehensive exhibitions of the 1990-95 Unzen eruptions. This museum is a core facility of Unzen Volcanic Area Global Geopark. The chronology of eruption, disasters from pyroclastic flows and lahars, USDP drilling project and video footage are displayed. We will see the overview of the Unzen eruption in this museum.

Stop 3-3: Unzen Lahar Memorial park

This area was affected by many lahar events during 1991-95 eruptions. Many houses and farm fields were buried extensively by lahar deposits. Some buried houses are preserved and exhibited in this Lahar Memorial park. Eleven houses were buried thickly in the deposits which are about 2.8 m thick.



Figure 35. Outcrop of the major pyroclastic flow deposits at Kita-Kamikoba area (Stop 3-4). June 3 and June 8 ash-cloud surge deposits, Sep. 15, 1991 and June 26, 1993 block-and-ash flow deposits are observed in this outcrop.

We plan to have early lunch in this park.

Stop 3-4: Kita-Kamikoba. Pyroclastic flow deposit and the memorial site

At stop 3-4 in Kita-Kamikoba, June 3 and June 8, ash-cloud surge deposits, Sep. 15, 1991 and June 26, 1993 block-and-ash flow and surge deposits are observed (Figs. 34, 35). A < 3.7 cm thick, 16:08 June 3, 1991 ash-cloud surge layer are seen at the



Figure 36. Outcrop of the major pyroclastic flow deposits (southeast of Stop 3-4; the columnar section at Minami-Kamikoba in Fig. 34). June 3 ash fall, June 8 ash-cloud surge deposits, Sep. 15, 1991 and June 26, 1993 block-and-ash flow deposits are observed in this outcrop.

bottom. A 5 cm thick, 19:51 June 8, 1991 ash-cloud surge layer consists of red-colored, normally graded, fine-grained ash. The 25 cm thick, sandy laminated, Sep. 15, 1991 surge layers consist of three units (16:44, 18:42, 18:54). A 19 cm thick, 01:15 June 26, 1993 block-and-ash flow layer is observed at the top. Thickness of the 16:08 June 3, 1991 ash-cloud surge is thin (a few cm to 30 cm), but it was quite destructive.

We visit the memorial site, where many people, including Maurice and Katia Krafft and Harry Glicken were killed by the surge. We also visit the Agricultural Training Center, where many firemen and police people were killed by the June 3, 1991 ash-cloud surge.

At the southeast of stop 3-4, Minami Kamikoba in the Mizunashi River, deposits of the June 3 ash fall beds, June 8 ash-cloud surge, Sep. 15, 1991 and June 26, 1993 block-and-ash flow are observed (Figs. 34, 36). A < 2 cm thick, red-colored deposit of the 16:08 June 3, 1991, fine ash fall is seen on the pre-eruption soil. A 12 cm thick, sandy

deposit of the 19:51 June 8, 1991 ash-cloud surge is also observed. The 16:44 Sep. 15, 1991 block-and-ash flow deposit consists of the lower 7 cm thick, fine grained sandy layer and the upper 150 cm thick, coarse, reverse-grading layer. A 35 cm thick deposit of the 17:59 Sep. 15 ash-cloud surge is fine-grained, red-colored, and reversely-graded. The 4 cm thick, 18:42 Sep. 15 ash-cloud surge layer consists of sandy materials, while the 18:54 Sep. 15 deposit consists of lower 37 cm thick, coarse grained, reverse-grading block-and-ash flow layer and upper 4 cm thick fine-grained, ash-cloud surge layer. The coarse grained layer contains many carbonized wood fragments. Above the thin layers between Sep. 1991 and June 1993, a 140 cm thick, 1:15 June 26, 1993 block-and-ash flow deposit consists of < 1 m size boulders, blocks, lapilli and ash is observed. Lahar deposits which formed after June 26, 1993 are observed at the top. In this stop, we examine the depositional features of these deposits and discuss the emplacement processes.

Lahar deposits consisting of up to few meter

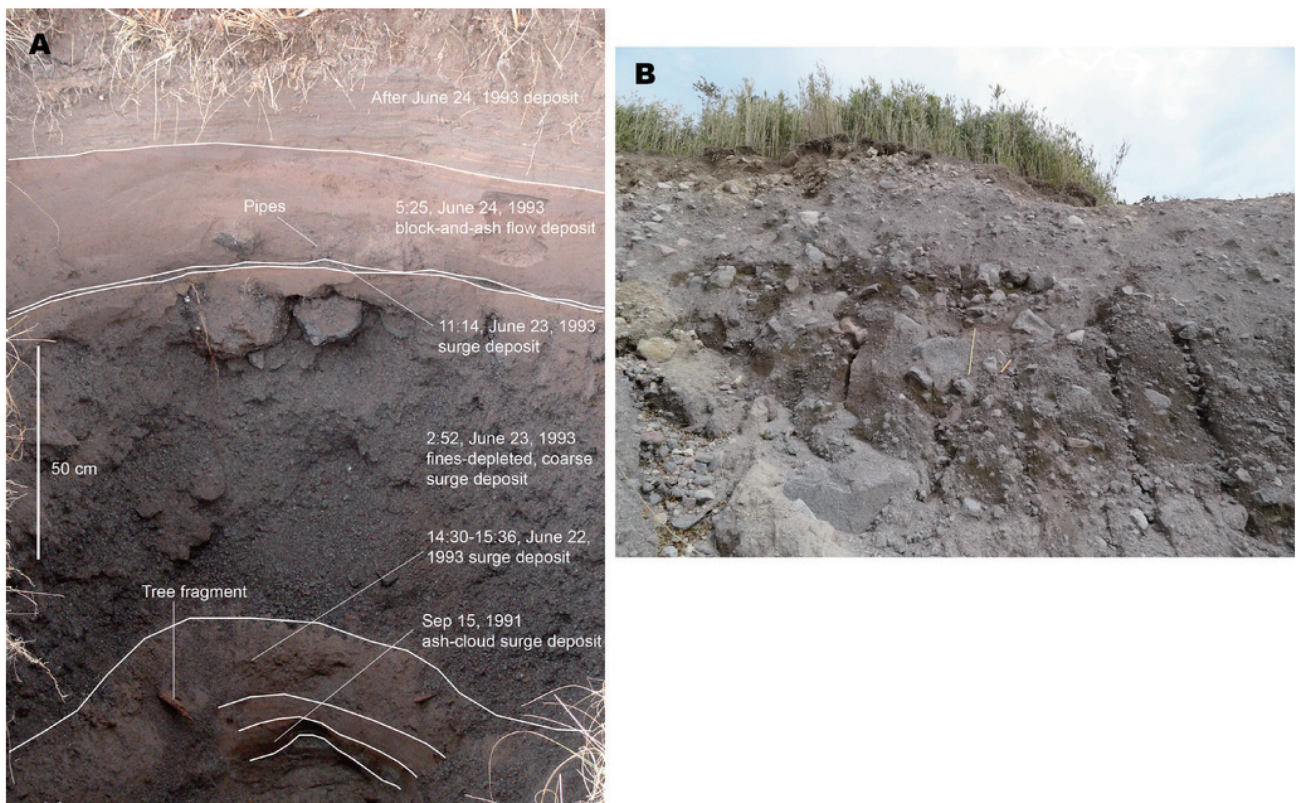


Figure 37. (A) Trench section at the Tarukidaichi (Taruki Height) (Stop 3-6', the columnar section B at Tarukidaichi in Fig. 34). Sep. 15, 1991 and June 22-24, 1993 block-and-ash flow, surge and fall deposits are observed in this trench section. (B) Tarukidaichi debris avalanche deposit comprised of block-and-ash flow and lahar deposits (Stop 3-6).

size (sometimes 10 m size), reversely graded, sub-rounded blocks and boulders are observed in the Mizunashi River. The deposits show partly stratified or laminated, usually fines-depleted, clast to matrix supported depositional features. Fine-grained, silt-size ash is relatively depleted compared to block-and-ash flow deposits.

Stop 3-5: Minami-Kamikoba Onokoba Elementary School, pyroclastic flow and lahar deposits

The bus stops at the Onokoba Elementary School. The Onokoba Elementary School was attacked by the Sep. 15, 1991 ash-cloud surge. We discuss the damage and effects on the building by the ash-cloud surge.

Stop 3-6: Tarukidaichi (Taruki Height). A lookout point for the Heisei-Shinzan lava dome and Tarukidaichi debris avalanche deposit

At this stop, there are good views of the Heisei-Shinzan lava dome. We can also look at the fault scarp that bounded the southern part of the Unzen graben. This stop is located at the western part of the Tarukidaichi. This site is at the curve point of the Oshigadani. Therefore, ash-cloud surges were separated from the Sep. 15, 1991 pyroclastic flow at this point (Fig. 19). June 22-24 pyroclastic flows/surges also devastated this area. We can observe deposits from the Sep. 15, 1991 and June 22-24, 1993 pyroclastic flow and surges (Figs. 34, 37A). At the base, 12 cm thick deposit from the Sep. 15, 1991 (16:44, 17:59, 18:42 and 18:54) ash-cloud surges are observed. A 14 cm thick deposit from the 14:30-15:36 June 22, 1993 surge consists of sandy ash to pebbly lapilli and contains many tree fragments. A 75 cm thick deposit from the 2:52 June 23, 1993 surge is fines-depleted and contains < 15 cm size sub-angular blocks, lapilli, and ash. A 2-3 cm thick deposit from the 11:14 June 23 surge consists of sand and ash, while the 20 cm thick deposit from the 5:25 June 24, 1993 block-and-ash flow consists of ash-rich matrix-supported blocks, lapilli and ash, with many segregation pipes. In this trench section, we will examine depositional features of block-and-ash flow and surge deposits and discuss their origin and emplacement

mechanism. Origin and formation processes of the coarse fines-depleted 2:52 June 23, 1993 surge deposit are one of the points of discussion. The pyroclastic flow bumped against the hill of the Tarukidaichi, then a kind of hydraulic jump may occurred, which produced sudden separation of the coarse grained fines-depleted surge from the main pyroclastic flow.

The Tarukidaichi debris avalanche deposit (ca. 20-25 ka, Myokendake Volcano stage) is observed at this outcrop (Fig. 37B). The deposit consists of < 1 m-size, dense andesite blocks, lapilli and ash. Jigsaw cracks are sometimes observed in the blocks. Soft deformation features are observed in the debris-avalanche matrix part. Upper part of the debris avalanche deposit consists of debris-avalanche blocks made of inclined captured debris flow deposits. Uppermost part of the Tarukidaichi consists predominantly of this debris avalanche deposit. Formation mechanism of the debris-avalanche blocks and debris-avalanche matrix and emplacement mechanism of the Tarukidaichi debris avalanche are the point of discussion.

Stop 3-7: Minami-Senbongi. A section of the June 1993 pyroclastic flow deposit

The area was inundated by pyroclastic flows and debris flows beginning in May 1993, when the growth direction of lava dome at the summit changed towards the northwest and the upper stream of Oshigadani nearly filled with pyroclastic flow deposits. The pyroclastic flows cascaded down the northern cliff of the Tarukidaichi and swept trees away from the western slope of the hill north of the Tarukidaichi.

In this outcrop, we can observe the June 22-24, 1993 block-and-ash flow and ash-cloud surge deposits (Figs. 34, 38). In ascending order, we can see the following deposits; 1) 33 cm thick, 14:30-15:36 June 22, 1993 block-and-ash flow; 2) 9 cm thick, 2:52 June 23 ash-cloud surge; 3) 10 cm thick, 11:14 June 23 ash-cloud surge; and 4) 175 cm thick, 5:25 June 24 block-and-ash flow deposit are observed. We will examine the depositional features and discuss emplacement processes of these deposits in detail.

Shin-yake lava flow is seen at the north. The Shin-yake lava flow was formed during the 1792 eruption. We will visit the front of the Shin-yake lava flow on the last day. Northern side of the 11th lava lobe is seen at the SW direction. The Tarukidaichi is seen at the south direction. Chijiwa normal fault is seen at the northern site. The Tarukidaichi is bounded by the fault scarps. The original height of the Tarukidaichi may be lower than the present level. Western slope of the Shichimenzan lava dome (4 ka, northern part of Mayuyama lava dome) is seen at the eastern direction. Shape of the Shichimenzan lava dome is asymmetric. Origin and the formation process is point of discussion. The Shichimenzan lava dome produced a Mutsugi pyroclastic (block-and-ash) flow, which will be visited at stop 5-3.

4-4. Day 4: New Lava Dome Climbing

Climbing the Heisei-Shinzan lava dome (the 1991-1995 lava dome) takes six hours roundtrip from Nitta Pass (ropeway station). The lava dome



Figure 38. Outcrop at the Minami-Senbongi area (Stop 3-7, Minami-Senbongi columnar section in Fig. 34). June 22-24, 1993 block-and-ash flow and ash-cloud surge deposits are observed in this outcrop.

surface is covered with lava blocks up to a few meters across, and there is no trail on the dome. It is important to walk carefully since walking on the lava blocks is very slippery and lava blocks move easily under your weight, please take extreme care during this walk.

Stop 4-1: Nita Pass

The Nita Pass is the entrance to the summit area of the Unzen volcano, including Heisei-Shinzan lava dome (Fig. 39). A huge Heisei-Shinzan lava dome, formed by the 1990-1995 eruptions, stands in front of you. Shimanomine lava dome (4-6 ka) can be seen. A ropeway runs on the steep wall of the Myoken caldera formed by sector collapse about tens of thousand years ago. Pyroclastic flow materials, formed by dome collapse during the eruptions, are deposited on the bottom of the Akamatsudani valley.

Stop 4-2: Steep margins of the Heisei-Shinzan Lava Dome

The steep margins of the Heisei-Shinzan lava dome are covered with talus deposits, which comprise sub-angular to sub-rounded lava blocks 0.5-3 m across. The lava blocks consist of biotite-hornblende dacite that is characterized by large plagioclase phenocrysts. At the lower part of the steep margins, grass grows between the lava blocks. A 0.5-hour of climbing on the steep margins will take you to the flat top of the dome. Boulders are sometimes unstable. Follow markers and climb



Figure 39. Southern view of the Heisei-Shinzan new lava dome from the viewpoint to the Nita Pass.

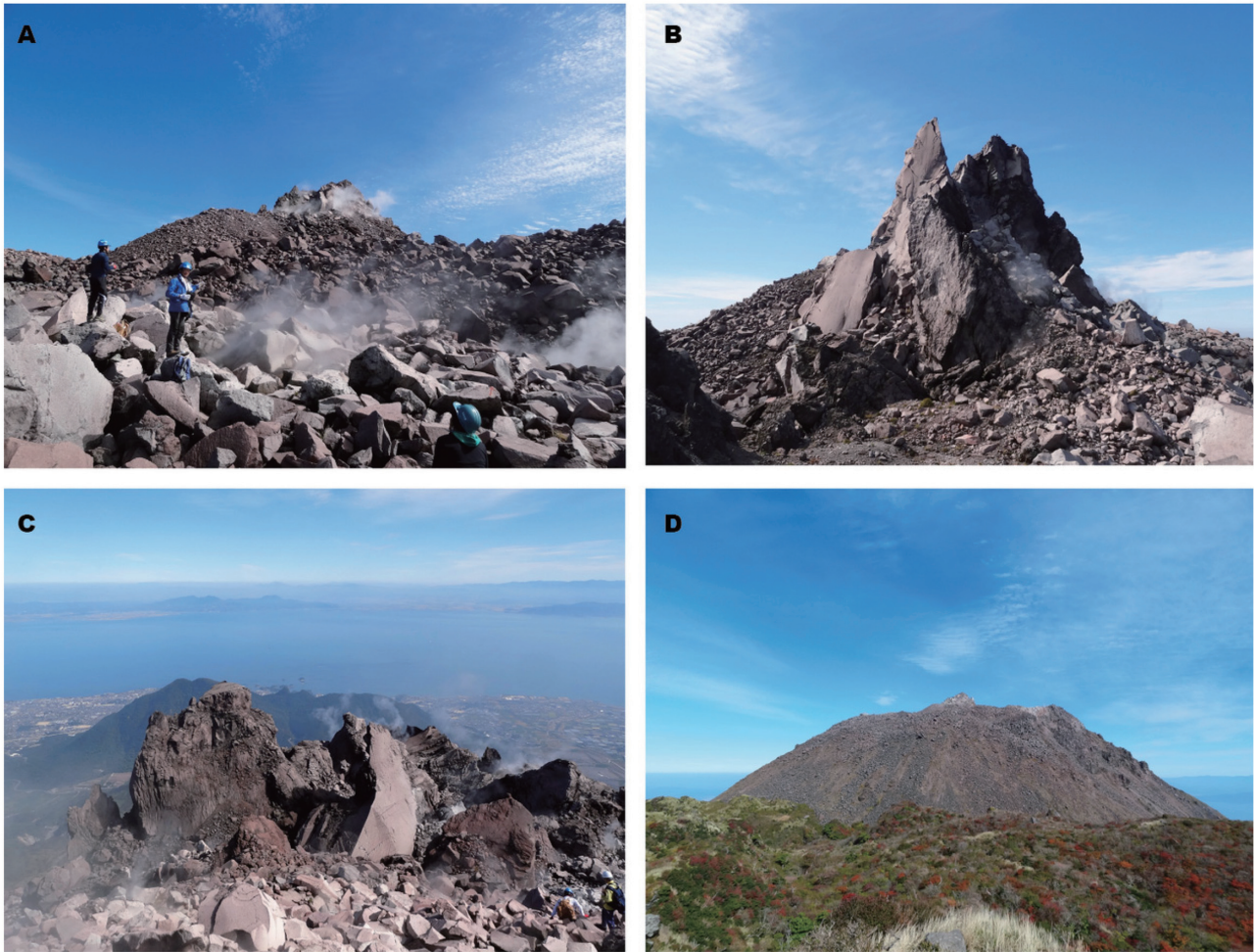


Figure 40. (A) Flat top of the Heisei-Shinzan lava dome covered with lava blocks. (B) Eastern view of spine of the Heisei-Shinzan lava dome (behind). (C) Surface features of 11th lobe. Behind is the Mayuyama Lava Dome and Ariake Sea. (D) Western view of the Heisei-Shinzan lava dome from the summit of Mount Fugen.

with cautions.

Stop 4-3: Flat top

This point provides an excellent view of the flat top of the Heisei-Shinzan lava dome (Fig. 40A). The surface of the flat top is covered with lava blocks. The lava blocks are mostly polyhedral with planar surfaces, and 0.5-5 m across. The surfaces of the lava blocks are reddish brown, smooth and commonly have contraction cracks that are arranged in octagonal or pentagonal, honeycomb patterns, 0.5-5 cm across. The interior of the lava blocks is massive and consists of poorly-vesicular, biotite-hornblende dacite. Mafic enclaves are seen in the lava. Some lava blocks have irregular fractures in the interior. Dacite along these fractures shows a highly vesicular texture. Large lava blocks 5-10 m across sporadically occur on the flat top. A lava

block has normal joints that are perpendicular to a curvilinear surface, and resembles prismatic jointed blocks.

Stop 4-4: Spine

The spine is elongated in east-west direction for 160 m, and is 30 m wide and 60 m high. Several fumaroles occur around the spine (Fig. 40B). The spine displays a massive core and brecciated rim. The massive core is 20 m wide and comprises coherent dacite. The dacite is uniform (non-flow banded), but bears a shear zone at the central part. The shear zone is 5 m wide, and the dacite within the zone show a cataclastic texture. The brecciated rim is < 5 m thick and well developed on the northern side of the spine. The breccia comprises angular clasts up to 1 m across and a finer matrix. Most clasts consist of unsheared dacite, but some

are composed of sheared dacite showing cataclastic texture. The cataclastic dacite also occur as blocks around the spine.

Stop 4-5: 11th lobe (Option)

The surface of the 11th lobe (Fig. 40C) is covered with lava blocks and coherent lavas. The lava blocks vary in diameter from 50 cm to several tens of meters, and more irregular in shape than those on the flat top. The coherent lavas show crease structures. These lava blocks and coherent lavas comprise variably vesiculated, biotite-hornblende dacite.

Stop 4-6: Summit of Mount Fugen

Mount Fugen (Fungendake) is an old lava dome formed within the Myoken caldera. The summit of Mount Fugen provides an excellent view of the Heisei-Shinzan lava dome (Fig. 40D). The lava dome is trapezoid with a flat top and steep margins. A spine projects at the center of the flat top. The thickness of the dome is 250 m. A carapace of lava blocks covers the flat top, and an apron of talus deposits has accumulated on the steep margins.

4-5. Day 5: Growth history of Unzen Volcano

Stop 5-1: Tateno. Kureishibaru pyroclastic flow deposit

The Kureishibaru pyroclastic flow deposit is a block-and-ash flow deposit of dacitic composition about 19 ka. In this stop, the deposit is composed of one to two flow units ranging in thickness about 0.5-1.5 m (Fig. 41). The deposit is clast-supported and is composed of angular to sub-rounded, fines-depleted, poorly-vesiculated lithic blocks, lapilli and a little ash. Imbrications of blocks are sometimes observed. Measurements of TRM (thermal remnant of magnetism) show high temperature during emplacement. The pyroclastic flow partly eroded lower soil and ash layers. This deposit interpreted to be formed by a collapse of lava dome, same as 1991-95 (Heisei) eruption. The thin deposit compared to other site (> 3-5 m) suggests a veneer-type (bank) deposit in this outcrop. Origin and formation processes of this fines-depleted pyroclastic flow deposit are the point of discussion. Several minor fault displacements are observed in the lower part of the deposit and soil



Figure 41. Kureishibaru pyroclastic flow deposit (19 ka) and minor fault displacement (1792AD). (Stop 5-1)

layer. These displacements are the result of numerous earthquakes during the 1792 eruption.

The AT (Aira-Tanzawa) ash fall (marker tephra at 29 ka derived from the Aira Caldera, southern Kyushu) is observed within the lower soil. The AT ash consists of bubble wall-type glass, occasionally containing 2-3 mm-size pumices.

Stop 5-2: Yakeyama. Front of the 1792 Shin-yake lava flow.

Front part of the 1792 Shin-yake block lava flow is exposed at this stop. The 1792 eruptions began with earthquakes and fumarolic activity, followed by outflow of the Shin-yake hornblende dacite lava flow northward for 2 km. Moving rate of the lava flow was ca. 30 m/day. Thickness of the Shin-yake lava flow is more than 50 m at the distal end. The dacite lava is one of the most acidic rocks in Unzen Volcano ($\text{SiO}_2 = 66\%$). Mafic enclaves are seen in the lava. This dacite lava flow was fluidal even though the SiO_2 contents were higher than the lava domes. Amount of microlites in the matrix are very small. Quite small amount of microlites may reduce the viscosity of the lava.

Stop 5-3: Kami-Orihashi. Mutsugi pyroclastic flow and Shimabara debris avalanche deposits

The Mutsugi pyroclastic flow deposit consists of dacite block-and-ash flows derived from the Shichimenzan lava dome. The deposit consists of a lower coarse-grained (up to 50 cm in diameter), fines-depleted, clast-supported unit and an upper finer-grained (up to 15 cm in diameter),

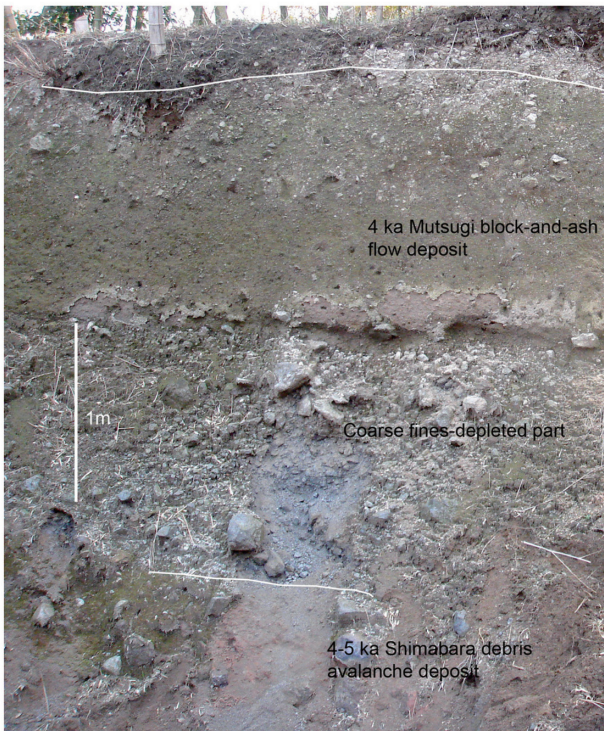


Figure 42. 4 ka Mutsugi block-and-ash flow deposit and 4-5 ka Shimabara debris avalanche deposit (Stop 5-3).



Figure 43. 1792 Mayuyama debris avalanche deposit at Chichibugaura Park (Stop 5-5).

matrix-supported unit (Fig. 42). TRM measurement of the lower unit show high temperature during emplacement. Charcoal in the deposits was dated at 4 ka by the ^{14}C method. The formation mechanism of the lower fines-depleted unit is a point of discussion. This Stop 5-3 is located at the higher part on the Chijiwa normal fault. Sudden separation from the main flow due to hitting against the steep wall may have occurred at this point. This process is similar to the coarse fines-depleted unit in the trench

section at the Tarukidaichi (Stop 3-6). Separation process between the upper and lower units is also point of discussion.

The Shimabara debris avalanche deposit is observed at the bottom of this outcrop. No soil is seen between the Mutsugi pyroclastic flow and the Shimabara debris avalanche deposits, suggesting the Shimabara debris avalanche occurred at 4-5 ka during the formation stage of the Shichimenzan lava dome. The Shimabara debris avalanche consists of Middle Unzen stage lavas. Source of the Shimabara debris avalanche is point of discussion. One possibility is that the Shichimenzan lava dome pushed up the Middle Unzen stage lava and unstable part of the Middle Unzen stage lava was collapsed, forming the Shimabara debris avalanche.

Stop 5-4: Nita Danchi. Amphitheater of the 1792 debris avalanche and lookout point

This is the lookout point of the 1792 Mayuyama debris avalanche deposit and the source Mayuyama lava dome. On May 21, 1792, an intense earthquake triggered a large-scale landslide at Tenguyama lava dome, causing the Mayuyama debris avalanche. We can observe many hummocks from this stop. Southern part of Shimabara City is developed on the Mayuyama debris avalanche deposit. Vertical wall (scar of the amphitheater) of the Tenguyama is seen. On the vertical wall, cooling cracks and conjugate tectonic joints are developed in the dacite lava dome.

This stop is located on the southern marginal levee of the avalanche deposit, where a 3 m-thick, debris avalanche deposit, is observed. Many jigsaw cracks are seen in the blocks. Jigsaw cracks are also observed in the deposit at 1 km east from the source. This suggests that jigsaw cracks were mainly formed during the early sliding stage (Takarada and Melendez, 2007).

Stop 5-5: Chichibugaura. 1792 debris avalanche deposit

Sections of the 1792 debris avalanche deposit are observed at this stop (Fig. 43). Debris-avalanche blocks in the 1792 debris avalanche deposit are homogeneous and vary in the degree of fragmentation. Less fragmented portions contain angular blocks with pervasive jigsaw cracks. Highly

fragmented parts look debris-avalanche matrix but we interpreted that these parts are still part of a debris-avalanche block. Stretched mafic enclaves are sometimes seen in the highly fractured dacite blocks. Fracturing and deformation processes in the debris-avalanche blocks and transportation mechanism of the debris avalanche are points of discussion.

Due to the weight of the overlying mass and underlying topographical variations, initiation of sliding occurred unequally throughout the mass resulting in shear stress-induced jigsaw cracks (Fig. 44). The sliding mass progressed as a laminar plug flow during the main stage of transport, preserving jigsaw cracks and angularity. Strong shear stress resulting from friction between the sliding mass and underlying basement concentrated along the margins and base, creating the debris-avalanche matrix during the acceleration stage. Debris-avalanche matrix continued to form during transport from shear stress and entrainment of basement. A dramatic decrease in slope angle caused the sliding mass to disaggregate laterally. After cessation of movement, unstable sections of the mass collapsed forming hummocks (Takarada and Melendez, 2007).

Summary

Aso Volcano is a composite volcanic system comprising Aso caldera and post-caldera central cones. The Aso caldera, 25 km north-south and 18 km east-west, was formed by four gigantic pyroclastic-flow eruptions of andesitic to rhyolitic magma from ca. 270 ka to 90 ka. The caldera-forming Aso pyroclastic-flow deposits are divided into four units: Aso-1 (270 ka), Aso-2 (140 ka), Aso-3 (120 ka) and Aso-4 (90 ka) in ascending order. Post-caldera central cones were formed soon after the last caldera-forming eruption (90 ka) and have produced large volumes of fallout tephra and lava flows. At least seventeen cones are visible on the surface, and the shapes and structures of the central cones vary depending on their chemistry, which ranges from basalt to rhyolite. Nakadake Volcano, which is the only active central cone, is one of the most active volcanoes in Japan. At the post-caldera cones, explosive eruptions have frequently occurred although they have been much smaller than the caldera-forming stage eruptions.

Unzen volcano is located in the tectonic graben

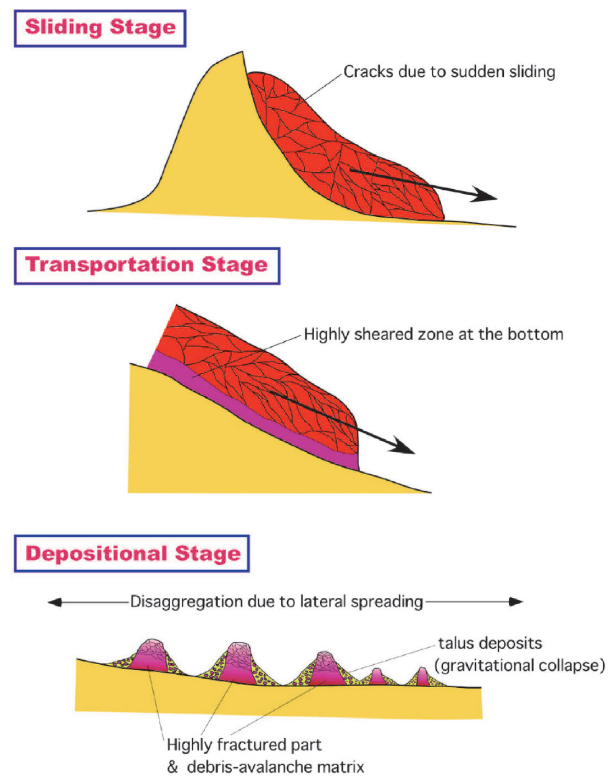


Figure 44. Initiation, transport and deposition mechanism of the 1792 Mayuyama debris avalanche.

of Shimabara Peninsula, Central Kyushu Japan. It covers a 20 km E-W and 25 km N-S area that consists of multiple lava domes, thick lava flows and pyroclastic deposits comprised of andesite and dacite. The volcanic activities of Unzen volcano can be divided into 3 stages; Older Unzen (0.5-0.3 Ma), Middle Unzen (0.3-0.15 Ma) and Younger Unzen (0.15- Ma) stages. Mayuyama lava dome that collapsed in 1792 caused a large-volume debris avalanche and tsunami that resulted to 15,000 fatalities. A new lava dome (Heisei-Shinzan) growth started since May 20, 1991 that made the 1.2 km long and 0.8 km wide (210 million m³ in DRE) lava dome complex. Intensive geophysical surveys revealed that a deep magma reservoir is located at 15-20 km depth beneath the Chijiwa bay, and the magma ascends obliquely eastwards with an inclination of 40-50 degrees. More than 9400 Merapi-type pyroclastic flows (block-and-ash flows) occurred from lava dome collapse during the 1991-95 Unzen eruptions. An ash cloud surge associated with a pyroclastic flow at 16:08 on June 3, 1991 killed 43 people, including Maurice and Katia Krafft and Harry Glicken. The largest pyroclastic flow occurred in Sep. 15, 1991.

Acknowledgements

We greatly appreciate Prof. Hiroshi Shimizu at Shimabara Volcano Observatory, Kyushu University and Setsuya Nakada at Earthquake Research Institute, University of Tokyo for their number of contributions and supports on this field trip.

References

- Fujii, T. and Nakada, S. (1999) The 15 September 1991 pyroclastic flows at Unzen Volcano (Japan): a flow model for associated ash-cloud surges. *J. Volcanol. Geotherm. Res.*, **89**, 159-172.
- Geological Survey of Japan (1992) 1:1,000,000 Geologic Map of Japan (3rd. ed.)
- Hashimoto, T. (1997) Self-potential changes and subsurface hydrothermal activity accompanying the 1990-1995 eruption of Unzen Volcano. *J. Geomag. Geoelectr.*, **49**, 977-993.
- Hoshizumi, H., Watanabe, K., Sakaguchi, K., Uto, K., Ono, K. and Nakamura, T. (1997) The Aso-4 pyroclastic flow deposit confirmed from the deep drill holes inside the Aso caldera. *Prog. Abst. Volcanol. Soc. Japan*, 1997, No.2, 5. (in Japanese)
- Hoshizumi, H., Uto, K. and Watanabe, K. (1999) Geology and eruptive history of Unzen volcano, Shimabara Peninsula, Kyushu, SW Japan. *J. Volcanol. Geotherm. Res.*, **89**, 81-94.
- Ikebe, S. and Fujioka, M. (2001) "Yunotani Catastrophe" of 1816, in Aso Volcano, southwest Japan: historical records of steam explosion. *Bull. Volcanol. Soc. Japan*, **46**, 147-163. (in Japanese with English abstract)
- Ishihara, K. (1993) Continuous magma supply inferred from discharge rate of magma and ground-deformation rate at Mt. Unzen, Japan. *Annu. Disas. Prev. Res. Inst., Kyoto Univ.*, **36(B1)**, 219-230. (in Japanese with English abstract)
- Japan Meteorological Agency (1991) National catalogue of the active volcanoes in Japan (second edition). Japan Meteorological Agency, 500p. (in Japanese)
- Kagiyama, T., Utada, H. and Yamamoto, T. (1999) Magma ascent beneath Unzen Volcano, SW Japan, deduced from the electrical resistivity structure. *J. Volcanol. Geotherm. Res.*, **89**, 35-42.
- Kawaguchi, T. and Namba, S. (1954) A study of the June Flood (1953) in Kyushu: erosion control (1. general), Aso district. *Bulletin of Government Forest Experimental Station*, **69**, 97-123. (in Japanese with English abstract)
- Kohno, Y., Matsushima, T. and Shimizu, H. (2008) Pressure sources beneath Unzen Volcano inferred from leveling and GPS data. *J. Volcanol. Geotherm. Res.*, **175**, 100-109.
- Kumamoto District Forest Office and Japan Forest Engineering Consultants (1991) Report of forest conservation project in the Aso region. 249p. (in Japanese)
- Machida, H. and Arai, F. (1983) Extensive ash falls in and around the Sea of Japan from large late Quaternary eruptions. *J. Volcanol. Geotherm. Res.*, **18**, 151-164.
- Machida, H. and Arai, F. (2003) Atlas of Tephra in and around Japan (revised edition). University of Tokyo Press, Tokyo 336 p. (in Japanese)
- Machida, H., Arai, F. and Momose, M. (1985) Aso-4 ash: a widespread tephra and its implications to the events of late Pleistocene in and around Japan. *Bull. Volcanol. Soc. Japan*, **30**, 49-70. (in Japanese with English abstract)
- Masuda, N., Watanabe, K. and Miyabuchi, Y. (2004) Rhyolite to dacite lava flows newly discovered on the western slope of Aso central cones, southwestern Japan. *Bull. Volcanol. Soc. Japan*, **49**, 119-128. (in Japanese with English abstract)
- Matsumoto, A., Uto, K., Ono, K. and Watanabe, K. (1991) K-Ar age determinations for Aso volcanic rocks – concordance with volcanostratigraphy and application to pyroclastic flows-. *Prog. Abst. Volcanol. Soc. Japan*, 1991, No.2, 73. (in Japanese)
- Miyabuchi, Y. (1999) Deposits associated with the 1990-95 eruption of Unzen volcano, Japan. *J. Volcanol. Geotherm. Res.*, **89**, 139-158.
- Miyabuchi, Y. (2009) A 90,000-year tephrostratigraphic framework of Aso Volcano, Japan. *Sedimentary Geology*, **220**, 169-189.
- Miyabuchi, Y. (2010) Eruption age of Komezuka at Aso Volcano, Japan. *Bull. Volcanol. Soc. Japan*, **55**, 219-225. (in Japanese with English abstract)
- Miyabuchi, Y. (2011) Post-caldera explosive activity inferred from improved 67-30 ka tephrostratigraphy at Aso Volcano, Japan. *J. Volcanol. Geotherm. Res.*, **205**, 94-113.
- Miyabuchi, Y. (2012) Landslides triggered by the July 2012 torrential rain in Aso caldera, southwestern Japan. *J. Geography*, **121**, 1073-1080. (in Japanese with English abstract)
- Miyabuchi, Y. and Daimaru, H. (2004) The June 2001 rainfall-induced landslides and associated lahars at Aso Volcano (southwestern Japan): implications for hazard assessment. *Acta Vulcanologica*, **16**, 21-36.

- Miyabuchi, Y. and Terada, A. (2009) Subaqueous geothermal activity revealed by lacustrine sediments of the acidic Nakadake crater lake, Aso Volcano, Japan. *J. Volcanol. Geotherm. Res.*, **187**, 140-145.
- Miyabuchi, Y. and Watanabe, K. (1997) Eruption ages of Holocene tephra from Aso volcano, southwestern Japan, inferred from ^{14}C ages of buried Andisols. *Bull. Volcanol. Soc. Japan*, **42**, 403-408. (in Japanese with English abstract)
- Miyabuchi, Y. and Watanabe, K. (2000) Phreatic explosions and ejecta around Jigoku spa, southwestern part of the central cones of Aso volcano. *Bull. Volcanol. Soc. Japan*, **45**, 25-32. (in Japanese with English abstract)
- Miyabuchi, Y., Hoshizumi, H., Takada, H., Watanabe, K. and Xu, S. (2003) Pumice-fall deposits from Aso volcano during the past 90,000 years, southwestern Japan. *Bull. Volcanol. Soc. Japan*, **48**, 195-214. (in Japanese with English abstract)
- Miyabuchi, Y., Hoshizumi, H. and Watanabe, K. (2004a) Late Pleistocene tephrostratigraphy of Aso Volcano, southwestern Japan, after deposition of AT ash. *Bull. Volcanol. Soc. Japan*, **49**, 51-64. (in Japanese with English abstract)
- Miyabuchi, Y., Masuda, N. and Watanabe, K. (2004b) Characteristics and age of eruption cycle producing Tateno lava at Aso Volcano, southwestern Japan. *Quaternary Res.*, **43**, 353-358. (in Japanese with English abstract)
- Miyabuchi, Y., Masuda, N. and Watanabe, K. (2004c) Geologic history of the western part of post-caldera central cones of Aso Volcano, southwestern Japan, based on stratigraphic relationships between lava flows and airfall tephra layers. *Bull. Volcanol. Soc. Japan*, **49**, 267-282. (in Japanese with English abstract)
- Miyabuchi, Y., Watanabe, K. and Egawa, Y. (2006) Bomb-rich basaltic pyroclastic flow deposit from Nakadake, Aso Volcano, southwestern Japan. *J. Volcanol. Geotherm. Res.*, **155**, 90-103.
- Miyabuchi, Y., Sugiyama, S. and Nagaoka, Y. (2012) Vegetation and fire history during the last 30,000 years based on phytolith and macroscopic charcoal records in the eastern and western areas of Aso Volcano, Japan. *Quaternary Int.*, **254**, 28-35.
- Miyoshi, M., Hasenaka, T., and Sano, T. (2005) Genetic relationships of the compositionally diverse magmas from Aso post-caldera volcanism. *Bull. Volcanol. Soc. Japan*, **50**, 269-283. (in Japanese with English abstract)
- Miyahara, T., Endo, K., Tohno, I., Chiba, T., Iso, N., Senda, K., Shinkawa, K., Yasui, M., Komori, J. and Ohno, M. (1992) Eruptive products of 1991 Unzen-Fugendake eruption (1). *Proc. Inst. Nat. Sci. Nihon Univ.*, **27**, 71-80. (in Japanese with English abstract)
- Nakada, S. and Fujii, T. (1993) Preliminary report on the activity at Unzen Volcano (Japan), November 1990-November 1991: dacite lava domes and pyroclastic flows. *J. Volcanol. Geotherm. Res.*, **54**, 319-333.
- Nakada, S., Miyake, Y., Sato, H., Oshima, O. and Fujinawa, A. (1995) Endogenous growth of dacite dome at Unzen volcano (Japan), 1993-1994. *Geology*, **23**, 157-160.
- Nakada, S., Shimizu, H. and Ohta, K. (1999) Overview of 1990-1995 eruptions at Unzen Volcano. *J. Volcanol. Geotherm. Res.*, **89**, 1-22.
- Nakamura, T. and Watanabe, K. (1995) Eruption deposits of Kishimadake and Ojodake volcanoes and black soil interbedded between tephra. *J. Kumamoto Geoscience Association*, **110**, 2-5. (in Japanese)
- Newhall, C. G. and Self, S. (1982) The Volcanic Explosivity Index (VEI): an estimate of explosive magnitude for historical volcanism. *J. Geophys. Res. (Oceans & Atmospheres)*, **87**, 1231-1238.
- Nishi, K. (2002) Three-dimensional seismic velocity structure beneath Unzen Volcano, Kyushu, Japan inferred by tomography from experimental explosion data. *Bull. Volcanol. Soc. Japan.*, **47**, 227-241.
- Nishi, K., Ono, H. and Mori, H. (1999) Global positioning system measurements of ground deformation caused by magma intrusion and lava discharge: the 1990-1995 eruption at Unzen volcano, Kyushu, Japan. *J. Volcanol. Geotherm. Res.*, **89**, 23-34.
- Ohta, K. (1997) Reviews on the prediction of the 1990-1995 eruption of Unzen Volcano and supporting system for risk management. *Bull. Volcanol. Soc. Japan*. **42**, 61-74. (in Japanese with English abstract)
- Okuno, M. (2002) Chronology of tephra layers in southern Kyushu, SW Japan, for the last 30,000 years. *Quaternary Res.*, **41**, 225-236. (in Japanese with English abstract)
- Ono, K. (1965) Geology of the eastern part of Aso caldera, central Kyushu, southwest Japan. *J. Geol. Soc. Japan*, **71**, 541-553. (in Japanese with English abstract)
- Ono, K. (1989) Rocks of Aso Volcano. Seminar of 1989 Fall Meeting of the Volcanological Society of Japan, 8-14. (in Japanese)

- Ono, K. and Watanabe, K. (1983) Aso caldera. *Gekkan Chikyu*, **44**, 73-82. (in Japanese)
- Ono, K. and Watanabe, K. (1985) Geological map of Aso volcano. Geological map of volcanoes 4, Geological Survey of Japan. (in Japanese with English abstract)
- Ono, K., Matsumoto, Y., Miyahisa, M., Teraoka, Y. and Kambe, N. (1977) Geology of the Taketa district. Geological Survey of Japan, 145p. (in Japanese with English abstract)
- Ono, K., Kubotera, A. and Ota, K. (1981) Aso volcano. In: A. Kubotera (ed.), "Field Excursion Guide to Sakurajima, Kirishima and Aso Volcanoes, Volcanological Society of Japan", 33-52.
- Ono, K., Shimokawa, K., Soya, T. and Watanabe, K. (1982) Geological and petrological study on the ejecta of 1979 eruption of Nakadake, Aso volcano, Japan. Report on an urgent study of 1979 eruption of Ontake and Aso volcano, Science and Technology Agency, 167-189. (in Japanese)
- Ono, K., Watanabe, K., Hoshizumi, H. and Ikebe, S. (1995) Ash eruption of the Naka-dake crater, Aso volcano, southwestern Japan. *J. Volcanol. Geotherm. Res.*, **66**, 137-148.
- Saito, E., Suto, S., Soya, T., Kazahaya, K., Kawanabe, Y., Hoshizumi, H., Watanabe, K. and Endo, H. (1993) Geodetic monitoring using EDM before and during the 1991-1992 lava extrusion of Fugen-dake, Unzen Volcano, Kyushu, Japan. *Bull. Geol. Surv. Japan*, **44**, 639-647. (in Japanese with English abstract)
- Shimizu, H. (1992) Monitoring of the eruptive activity at Unzen Volcano. *Butsuri-Tansa*, **45**, 458-466. (in Japanese with English abstract)
- Shimizu, H., Matsumoto, S., Uehira, K., Matsuwo, N. and Ohnishi, M. (2002) Seismic experiment for surveying the volcanic conduit of Unzen Volcano, using controlled sources. *Abst. 2002 Japan Earth Planet. Sci. Joint Meeting*, V054-014. (in Japanese with English abstract)
- Sparks, R. S. J., Self, S. and Walker, G. P. L. (1973) Products of ignimbrite eruptions. *Geology*, **1**, 115-118.
- Suzuki-Kamata, K. and Kamata, H. (1990) The proximal facies of the Tosu pyroclastic-flow deposit erupted from Aso caldera, Japan. *Bull. Volcanol.*, **52**, 325-333.
- Takarada, S. and Melendez, C. (2006) Depositional features and transport mechanism of the 1991-95 Unzen block-and-ash flows, Japan. Cities on Volcanoes 4. Quito Ecuador.
- Takarada, S. and Melendez, C. (2007) Comparison between emplacement mechanism of 1991-95 block-and-ash flows and 1792 Mayuyama debris avalanche at Unzen Volcano, Japan. IUGG 2007 Perugia, Italy.
- Takarada, S., Kazahaya, K., Kawanabe, Y., Sakaguchi, K., Suto, S., Yamamoto, T., Soya, T. and Unzendake Weather Station (1993a) Volume estimation of 1991-92 eruption of Unzen Volcano, and initiation mechanism of pyroclastic flows on June 3 and June 8, 1991. *Bull. Geol. Surv. Japan*, **44**, 11-24. (in Japanese with English abstract)
- Takarada, S., Yamamoto, T., Nakano, T., Murata, Y., Kazahaya, K., Kawanabe, Y., Sakaguchi, K. and Soya, T. (1993b) Computer simulations of pyroclastic flows of the 1991-92 eruption of Unzen Volcano. *Bull. Geol. Surv. Japan*, **44**, 25-54. (in Japanese with English abstract)
- Takarada, S., Hoshizumi, H., Nakada, S., Shimizu, H., Matsushima, T., Miyabuchi, Y., Yoshimoto, M., Goto, Y., Sugimoto, T. and Nagai, D. (2007) C1: Unzen Volcano and New Lava Dome Climb. Field Trip Guidebook, Cities on Volcanoes 5 Conference. Volcanological Soc. of Japan, 32p.
- Terada, A., Hashimoto, T., Kagiya, T. and Sasaki, H. (2008) Precise remote-monitoring technique of water volume and temperature of a crater lake in Aso volcano, Japan: implications for a sensitive window of a volcanic hydrothermal system. *Earth Planets Space*, **60**, 705-710.
- Uhira, K., Yamasato, H., Hashimoto, T., Fukui, K. and Takeo, M. (1995) Source mechanism of low-frequency seismic events at Unzen Volcano, Kyushu, Japan. *Bull. Volcanol. Soc. Japan*, **40**, 311-328.
- Umakoshi, K., Shimizu, H. and Matsuwo, N. (1994) Magma ascent path in the 1990-94 eruption of Fugendake, Unzen Volcano, as inferred from precisely determined hypocentral distribution. *Bull. Volcanol. Soc. Japan*, **39**, 223-235. (in Japanese with English abstract)
- Umakoshi, K., Shimizu, H. and Matsuwo, N. (2001) Volcano-tectonic seismicity at Unzen Volcano, Japan, 1985-1999. *J. Volcanol. Geotherm. Res.*, **112**, 117-131.
- Umakoshi, K., Shimizu, H. and Matsuwo, N. (2002) Seismic activity associated with the growth of the lava dome at Unzen Volcano (November 1993 - January 1994) - Grouping of earthquakes on the basis of cross-correlations among their waveforms-. *Bull. Volcanol. Soc. Japan*, **47**, 43-55. (in Japanese with English abstract)
- Uto, K., Sakaguchi, K., Shibuya, A. and Yoshioka, H. (1994) K-Ar ages of volcanic rocks from the deep drill holes inside the Aso caldera: implication for the

- reconstruction of the early stage of the post-caldera volcanism. *Prog. Abst. Volcanol. Soc. Japan* 1994, No.2, 211. (in Japanese)
- Watanabe, K. (1978) Studies on the Aso pyroclastic flow deposits in the region of the west of Aso caldera, southwest Japan, I: Geology. *Mem. Fac. Educ., Kumamoto Univ., Natural Science*, **27**, 97-120. (in Japanese with English abstract)
- Watanabe, K. (2001) Geology of Aso volcano. Ichinomiya Choshi (history of Ichinomiya town, Kumamoto prefecture, Japan), 7, 238p. (in Japanese)
- Watanabe, K. and Ono, K. (1992) Aso volcano. In: T. Yanagi, S. Nakada and Watanabe, K., "Active volcanoes and geothermal systems in the rift zone in middle Kyushu", the 29th IGC field guide book, 226-229.
- Watanabe, K. and Hoshizumi, H. (1995) Geological Map of Unzen volcano. Geological Map of Volcanoes **8**, Geological Survey of Japan. (in Japanese with English abstract)
- Watanabe, K., Danhara, T., Watanabe, K., Terai, K. and Yamashita, T. (1999) Juvenile volcanic glass erupted before the appearance of the 1991 lava dome, Unzen volcano, Kyushu, Japan. *J. Volcanol. Geotherm. Res.*, **89**, 113-121.
- Yamamoto, T., Takarada, S. and Suto, S. (1993) Pyroclastic flows from the 1991 eruption of Unzen volcano, Japan. *Bull. Volcanol.*, **55**, 166-175.
- Yamasato, H. (1999) Nature of infrasonic pulse accompanying low frequency earthquake at Unzen volcano. *Bull. Volcanol. Soc. Japan*, **43**, 1-13.
- Yamashina, K. and Shimizu, H. (1999) Crustal deformation in the mid-May 1991 crisis preceding the extrusion of a dacite lava dome at Unzen Volcano, Japan. *J. Volcanol. Geotherm. Res.*, **89**, 43-55.